



DIGITAL ACCESS TO SCHOLARSHIP AT HARVARD

Paired Electron Pockets in the Hole-Doped Cuprates

The Harvard community has made this article openly available.
[Please share](#) how this access benefits you. Your story matters.

Citation	Galitski, Victor, and Subir Sachdev. 2009. Paired electron pockets in the hole-doped cuprates. <i>Physical Review B</i> 79(13): 134512.
Published Version	doi:10.1103/PhysRevB.79.134512
Accessed	February 19, 2015 9:13:11 AM EST
Citable Link	http://nrs.harvard.edu/urn-3:HUL.InstRepos:7696990
Terms of Use	This article was downloaded from Harvard University's DASH repository, and is made available under the terms and conditions applicable to Open Access Policy Articles, as set forth at http://nrs.harvard.edu/urn-3:HUL.InstRepos:dash.current.terms-of-use#OAP

(Article begins on next page)

Paired electron pockets in the hole-doped cuprates

Victor Galitski

*Joint Quantum Institute and CNAM, Department of Physics,
University of Maryland, College Park, MD 20742-4111*

Subir Sachdev

Department of Physics, Harvard University, Cambridge MA 02138

(Dated: December 30, 2008)

Abstract

We propose a theory for the underdoped hole-doped cuprates, focusing on the “nodal-anti-nodal dichotomy” observed in recent experiments. Our theory begins with an ordered antiferromagnetic Fermi liquid with electron and hole pockets. We argue that it is useful to consider a quantum transition at which the loss of antiferromagnetic order leads to a hypothetical metallic “algebraic charge liquid” (ACL) with pockets of charge $-e$ and $+e$ fermions, and an emergent U(1) gauge field; the instabilities of the ACL lead to the low temperature phases of the underdoped cuprates. The pairing instability leads to a superconductor with the strongest pairing within the $-e$ Fermi pockets, a d -wave pairing signature for electrons, and very weak nodal-point pairing of the $+e$ fermions near the Brillouin zone diagonals. The influence of an applied magnetic field is discussed using a proposed phase diagram as a function of field strength and doping. We describe the influence of gauge field and pairing fluctuations on the quantum Shubnikov-de Haas oscillations in the normal states induced by the field. For the finite temperature pseudogap region, our theory has some similarities to the phenomenological two-fluid model of $-2e$ bosons and $+e$ fermions proposed by Geshkenbein, Ioffe, and Larkin [Phys. Rev. B **55**, 3173 (1997)], which describes anomalous aspects of transverse transport in a magnetic field.

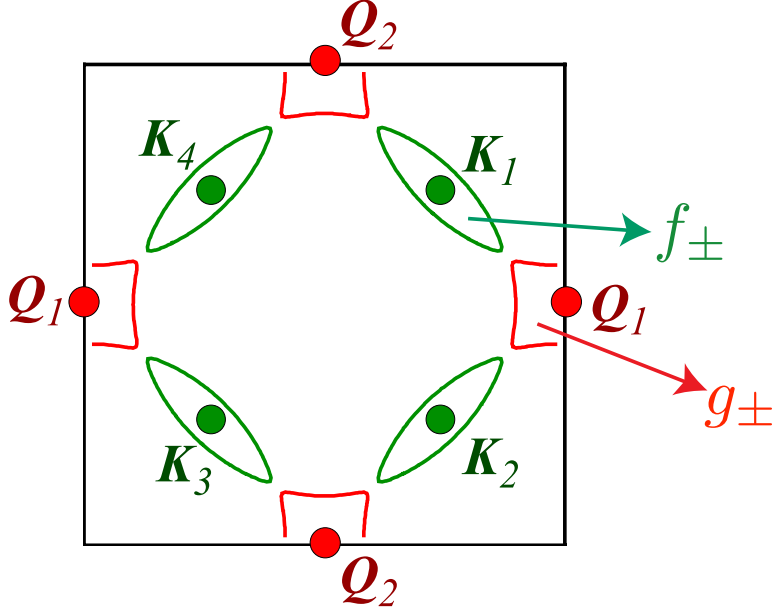


FIG. 1: Square lattice Brillouin zone map showing the electron and hole pockets of conventional spin density wave theory^{10,11,12,13} of antiferromagnetic order at wavevector (π, π) . The hole pockets are centered at the wavevectors $\mathbf{K}_v = (\pm\pi/2, \pm\pi/2)$ (where $v = 1 \dots 4$), and the electron pockets are centered at $\mathbf{Q}_a = (\pi, 0), (0, \pi)$ (where $a = 1, 2$). The present paper describes the influence of quantum and thermal fluctuations in the orientation of the antiferromagnetic order on the electron and hole pockets. We will find strong pairing of the electron pockets at \mathbf{Q}_a , which induces a weak ‘proximity effect’ pairing of the hole pockets at \mathbf{K}_v , with all the pairings consistent with a $d_{x^2-y^2}$ pairing signature.

I. INTRODUCTION

A remarkable consensus has emerged in recent experiments^{1,2,3,4,5,6,7,8,9} on the enigmatic underdoped region of the hole-doped cuprate superconductors. These experiments reveal a clear “dichotomy” between the low-lying electronic excitations near the nodal points of the d -wave superconductor (*i.e.* near the wavevectors \mathbf{K}_v in Fig. 1) and the higher energy excitations near the “anti-nodal” points (*i.e.* near the wavevectors \mathbf{Q}_a in Fig. 1). The nodal quasiparticles have a pairing energy which decreases with decreasing doping, and they form coherent quasiparticles which display characteristic interference patterns in scanning tunneling microscopy (STM) observations. In contrast, the anti-nodal excitations have a larger gap which increases with decreasing doping, and they appear to be excitations of a state with STM modulations characteristic of a valence bond solid.⁵

Theoretically, a number of numerical studies^{14,15,16} of the Hubbard model have also presented evidence for the nodal-anti-nodal dichotomy at intermediate energy scales. These results are connected to ad hoc theoretical models^{17,18,19,20} involving “Fermi arc” and/or electron/hole pockets which violate the traditional Luttinger theorem on the area enclosed by the Fermi surfaces. A central point behind the analysis of the present paper is that

theories with such ad hoc violations of the Luttinger Fermi area law are fundamentally incomplete. Using arguments building upon the non-perturbative proof of the Luttinger theorem,²¹ it was argued^{22,23} that metallic states with non-Luttinger Fermi surfaces must have “topological order,” by which we mean there must be additional collective excitations associated with an emergent gauge field. Such collective excitations are crucial in the description of such exotic conducting states. Specific theories^{24,25,26} of conducting states with non-Luttinger areas, labeled “algebraic charge liquids” (ACL), have been provided: in models appropriate for the cuprates, these states were obtained across quantum transitions involving the loss of antiferromagnetic Néel order. Furthermore, the formalism developed to describe the quantum ACL is also useful for describing the “liquid” state obtained when the antiferromagnetic order is lost by thermal fluctuations.

We begin presentation of our results by recalling spin-density-wave (SDW) studies of the onset of antiferromagnetic order in the doped cuprates.^{10,11} These works are expressed in terms of a vector SDW order parameter N_ℓ (with $\ell = x, y, z$), measuring the spin-density-wave at wavevector (π, π) , which can perturb the Fermi surface of a weak-coupling band structure; we will restrict our attention here to the commensurate Néel SDW, and recent work by Harrison¹³ has shown that a similar Fermi surface structure is obtained for incommensurate SDW order. The theory for the transition from the SDW ordered state ($\langle N_\ell \rangle \neq 0$) to the non-magnetic state ($\langle N_\ell \rangle = 0$) is expressed in terms of an effective action for space-time fluctuations N_ℓ . The state with $\langle N_\ell \rangle \neq 0$ has “small” Fermi pockets: hole pockets centered at the \mathbf{K}_v and electron pockets centered at the \mathbf{Q}_a . This conventional, ordered antiferromagnetic state will also be present in our theory below. In the spin-density-wave theory, the non-magnetic state with $\langle N_\ell \rangle = 0$ has a “large” Fermi surface which obeys the conventional Luttinger theory, and the transition from the small Fermi pockets state to a “large” Fermi surface *co-incides* with the loss of SDW order.

In our theory below, the physical properties of the SDW ordered state are qualitatively identical to those in the spin-density-wave theory. However, we express our theory for the loss of SDW order not in terms of the vector N_ℓ order parameter, but in terms of a bosonic spinor z_α which is related to N_ℓ by

$$N_\ell = z_\alpha^* \sigma_{\alpha\beta}^\ell z_\beta, \quad (1.1)$$

where the σ^ℓ are the Pauli matrices. Then, the state with $\langle z_\alpha \rangle \neq 0$ is the same as the spin-density wave state with $\langle N_\ell \rangle \neq 0$. However, an important advantage of the formulation in terms of the z_α is that we can describe the electron spin in terms of its components quantized along the direction of the local Néel order, simply by performing a SU(2) rotation defined by the spinor z_α . This facilitates a description of the non-magnetic state^{24,25,26} with $\langle z_\alpha \rangle = 0$, which is a topologically ordered ACL that retains key aspects of the “small” Fermi surface structure, as summarized in Fig. 2, and will be discussed in detail below. The z_α formalism also efficiently describes the non-magnetic state obtained when SU(2) invariance is restored

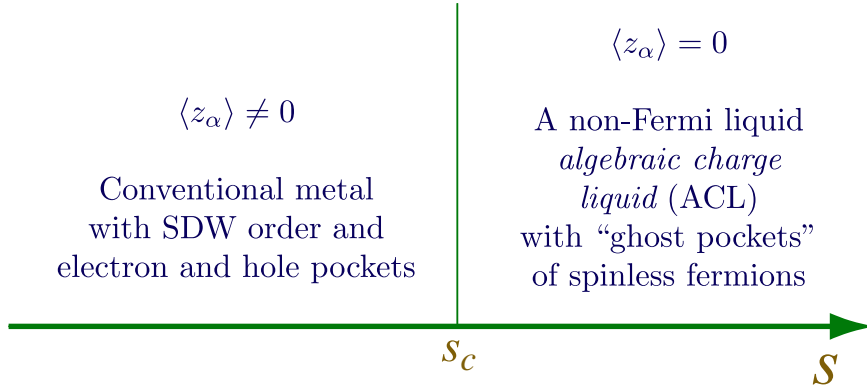


FIG. 2: Non-superconducting ground states of our theory as a function of the coupling s which tunes the strength of the SDW fluctuations (see \mathcal{L}_z in Eq. (A1)); s is controlled by varying the doping δ and by choosing different cuprate series. We expect that at zero applied magnetic field, H , these phases are pre-empted by superconductivity; the phase diagram as a function of H and δ is shown in Fig. 3.

by thermal fluctuations.

The primary motivation for the present paper comes from the recent experimental evidence for electron pockets in the hole doped cuprates at large magnetic fields: Shubnikov-de Hass (SdH) and de Hass-van Alphen (dHvA) oscillations^{27,28,29,30,31} indicate carriers in small pockets, and Hall conductivity measurements³² have been used to argue that these are electron pockets. One of our main claims is that an algebraic charge liquid consisting of a pocket of charge $-e$ fermions at the \mathbf{Q}_a wavevectors, and of charge $+e$ fermions at the \mathbf{K}_v wavevectors, provides the underlying quantum state for the description of the underdoped cuprates, and also for the thermal fluctuations of the more classical liquid state in the ‘pseudogap’ regime. Speculations along these lines were also made in Ref. 26. This ACL preserves the full symmetry of the Hamiltonian. Instabilities of this ACL involving the onset of SDW order, superconductivity, and charge order will be key for the description of the underdoped regime — see the proposed phase diagram in Fig. 3. In particular, the onset of superconductivity removes low energy fermionic excitations which suppress monopole-instantons in the gauge field, and so is likely to lead to a confinement transition; this confinement physics has been studied in model systems in earlier work²⁶, and we will not discuss it further here.

We shall pay particular attention here to the pairing of the $-e$ pocket. We note that a phenomenological model of pairs of electrons near the \mathbf{Q}_a wavevectors, with charge $-2e$, was considered by Geshkenbein, Ioffe, and Larkin,¹⁷ and we will discuss the connection to their model further in Section II. As we will describe there, the charge carriers in this pocket experience a strong attractive interaction, which causes them to form an s -wave paired state. However, the resulting superconducting state actually has d -wave pairing for the physical electrons,²⁶ as will be reviewed in Section II. Furthermore, we will show that the pairing of the fermions near the \mathbf{K}_v wavevectors is very weak, and has nodal points along the Brillouin

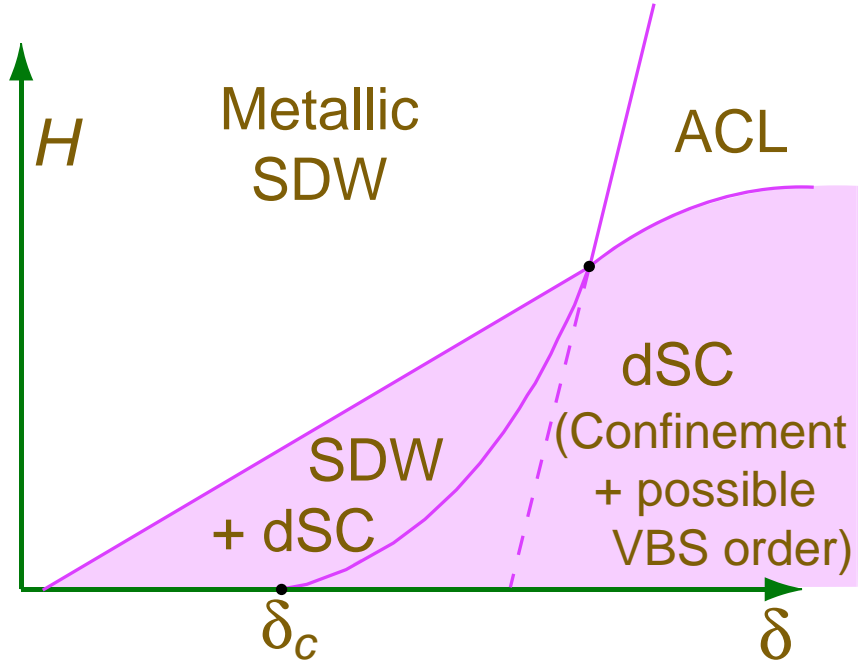


FIG. 3: Proposed zero temperature phase diagram for the underdoped cuprates as a function of doping, δ , and a magnetic field H perpendicular to the layers; the insulating phases at very small δ are not shown. This phase diagram combines our present results with those of Refs. 10 and 34. The value of δ_c , and the scale of δ will be differ for the various cuprate series. The superconducting phases are shaded and labeled dSC. The dashed line indicates the normal state phase boundary of Fig. 2 which is pre-empted by the onset of superconductivity. The physics of the confinement and possible valence bond solid (VBS) order in the dSC state is discussed in Ref. 26. At higher δ , there is a transformation to the physics of the “large” Fermi surface state, which we do not describe here. Only the ACL phase above has unconventional ‘topological’ order; all other phases have conventional order and associated excitations. While the ACL can be a stable ground state at large H , it is possible it is pre-empted by a conventional Fermi liquid.

zone diagonals. Thus our theory contains a low density of strongly paired charge carriers, a d -wave pairing signature with nodal points, and a nodal-anti-nodal dichotomy: these are all attractive phenomenological features.

We shall describe the loss of superconductivity in this state by an applied magnetic field, H , and the appearance of SdH oscillations at $H > H_{c2}$, using the phase diagram in Fig. 3. Both the SDW metal and the ACL metal exhibit SdH oscillations. Specific predictions for the H and temperatures (T) dependence of these SdH oscillations will be provided, which can potentially be compared with experiments. Because our charge $\pm e$ fermions do not carry spin, a key feature of the SdH oscillations will be the absence of a linear Zeeman splitting in the Fermi surface areas, both in the ACL and in the phase with SDW order.³³

Another effect of the applied H field is that it can induce or enhance the SDW order for the fields at which superconductivity is present — see Fig. 3. This has been discussed

theoretically in some detail,³⁴ and in Section II we will show that our present pairing theory provides a specific mechanism for the competition between antiferromagnetism and superconductivity. This field-induced enhancement of SDW order is also clearly observed in the La series of hole-doped cuprates.^{35,36,37,38,39,40} The samples with $\delta = 0.1$ display³⁶ the behavior expected for $\delta < \delta_c$; the samples with $\delta = 0.144$ have observed^{38,39,40} the physics predicted³⁴ for $\delta > \delta_c$, including the dSC to dSC+SDW transition at a non-zero H . Thus for the La compounds we expect that δ_c is between the quoted values. Very recently, field induced SDW order characteristic of $\delta > \delta_c$ has also been reported⁴¹ for $\text{YBa}_2\text{Cu}_3\text{O}_{6.45}$. The quantum oscillation experiments^{27,28,29,30,31,32} are on the same (or closely related) compound, and so it is plausible that they are in the metallic SDW phase of Fig. 3, as others have also suggested.⁴² Our predictions for quantum oscillations and pairing instabilities will also extend to this metallic SDW phase.

Our theory also offers a natural starting point for a description of the finite T “pseudogap” region of the underdoped cuprates. The strongly paired $-e$ pockets lead to an effective description in terms of charge $-2e$ bosons which can exist above the superconducting critical temperatures.¹⁷ After a duality mapping, this leads to a theory of a vortex liquid which can capture both the “phase” fluctuations and the possible instabilities to varieties of charge order.^{43,44} We will explore some of the thermoelectric transport properties of such a model in Section IV.

The physics of the lightly-doped Mott insulator as described by a t - J model is usually implicated in the description of cuprate superconductivity.⁴⁵ From this perspective, our use, following a proposal in Ref. 26, of charge $-e$ carriers for the hole-doped cuprates may seem unacceptable. It is often argued that such excitations are only present across a Hubbard gap of energy U , and the limit $U \rightarrow \infty$ has been taken by a Gutzwiller projection of such carriers.⁴⁵ In response to this potential objection, we have the following responses:

(i) We draw the reader’s attention to the electron-doped cuprates, which presumably have a similar value of U , and for which *both* electron-like and hole-like carriers have been observed in photoemission experiments on the state with SDW order.^{46,47,48,49} We are assuming here that similar physics applies to the hole-doped cuprates.

(ii) While the upper Hubbard band is indeed separated by an energy of order U , a “Kondo resonance” of these states can be present at the Fermi level, and this is described by our charge $-e$ carriers. Indeed states from both the upper and lower Hubbard bands are required^{26,50} for the eventual appearance of the Fermi-liquid Luttinger (“large”) Fermi surface state in the overdoped regime, and so we claim it is not surprising that both bands have precursors in the underdoped regime.

(iii) We note recent arguments by Comanac *et al.*,⁵¹ based upon optical conductivity data and dynamic mean field theory arguments, that the effective U in the hole-doped cuprates is not as large as is commonly assumed.

(iv) As we will review below, the electron pockets reside in a region of the Brillouin zone where the pairing force is strongest. Thus for these momenta, it will pay to acquire states

from the upper Hubbard band to benefit from the increased pairing energy. The effective density of carriers in the charge $-e$ pockets will be larger than would have been assumed without accounting for the pairing. Indeed, even if the chemical potential is below the bottom of the band of $-e$ carriers, the pairing interaction will induce a non-zero density of $-e$ carriers.

The outline of the remainder of our paper is as follows. In Section II, we describe our model for the underdoped cuprates. The primary actors are the electron pockets near \mathbf{Q}_a which pair strongly. We show how this model leads naturally to a d -wave superconducting pairing for physical electrons, with only weak pairing and nodal excitations along the zone diagonals near the \mathbf{K}_v points. Section III will consider quantum oscillations in the normal state obtained by applying a strong magnetic field. We will describe the corrections to the Lifshitz-Kosevich formula from gauge field and pairing fluctuations. Section IV will discuss additional experimental consequences of our theory: a two-fluid model for transverse thermoelectric transport in the pseudogap region.

II. THE MODEL

The starting point of our analysis is an expression^{24,25,26} for the electron annihilation operator $\Psi_\alpha(\mathbf{r})$ (where $\alpha = \uparrow, \downarrow$ is a spin index) in terms of continuum fermionic fields $F_{v\alpha}$ and $G_{a\alpha}$, which reside in the vicinity of the wavevectors \mathbf{K}_v and \mathbf{Q}_a respectively:

$$\Psi_\alpha(\mathbf{r}) = \sqrt{Z_f} \sum_{v=1}^4 e^{i\mathbf{K}_v \cdot \mathbf{r}} F_{v\alpha}^\dagger + \sqrt{Z_g} \sum_{a=1}^2 e^{i\mathbf{Q}_a \cdot \mathbf{r}} G_{a\alpha}. \quad (2.1)$$

Here $Z_{f,g}$ are non-singular quasiparticle renormalization factors which depend upon microscopic details. As will be described explicitly below, the fermions $F_{v\alpha}$ and $G_{a\alpha}$ are in turn expressed in terms of a bosonic spinon field z_α , and spinless fermions which carry the electromagnetic charge. The phases with $\langle z_\alpha \rangle \neq 0$ have been shown²⁵ to be conventional SDW-ordered states:^{10,11} the excitation spectrum co-incides with that obtained in spin-wave/Hartree-Fock theory. However, the utility of the parameterizations below is that the same formalism can be easily extended across the quantum transition at which Néel order is lost, and we reach a phase with $\langle z_\alpha \rangle = 0$. There is substantial recent numerical evidence^{52,53,54,55} that the z_α -based theory correctly captures the low energy fluctuations across the Néel-disordered transition in insulating model systems. One of our main assumptions will be that this description in terms of the z_α is a valid starting point for describing the loss of Néel order in the doped cuprates. The theory for this Néel disordering transition also involves an emergent U(1) gauge field $A_\mu \equiv (A_\tau, \mathbf{A})$, which is connected to the gauge field of the CP¹ model; the z_α carry unit charge under A_μ . Here μ is a spacetime index extending over the spatial co-ordinates x, y and the imaginary time co-ordinate τ .

For the electronic excitations near the \mathbf{K}_v , we need the electromagnetic charge $+e$ “holon”

annihilation operators f_{qp} , where $q = \pm$ and $p = 1, 2$. Here q is the “charge” under A_μ , and p is a “valley” index; note that although there are 4 pockets near the \mathbf{K}_v in Fig. 1, a proper counting of degrees of freedom requires only two valleys. The complete expressions for the $F_{v\alpha}$ at all for \mathbf{K}_v points in terms of the $f_{\pm p}$ are²⁴

$$\begin{pmatrix} F_{1,2\uparrow}^\dagger \\ F_{1,2\downarrow}^\dagger \end{pmatrix} = \mathcal{R}_z \begin{pmatrix} f_{+1,2}^\dagger \\ -f_{-1,2}^\dagger \end{pmatrix} \quad , \quad \begin{pmatrix} F_{3,4\uparrow}^\dagger \\ F_{3,4\downarrow}^\dagger \end{pmatrix} = \mathcal{R}_z \begin{pmatrix} f_{+1,2}^\dagger \\ f_{-1,2}^\dagger \end{pmatrix}, \quad (2.2)$$

where

$$\mathcal{R}_z \equiv \begin{pmatrix} z_\uparrow & -z_\downarrow^* \\ z_\downarrow & z_\uparrow^* \end{pmatrix}. \quad (2.3)$$

The physical content of this parameterization is simple: the \pm indices of the $f_{\pm p}$ are the spin components quantized along the local SDW order, and these are rotated by the SU(2) matrix \mathcal{R}_z to a fixed quantization direction by the z_α . Note that pockets separated by the SDW ordering wavevector of (π, π) are parameterized by the same degrees of freedom, and they differ only sign of the f_{-v} operator. Eq. (2.2) is the same as the parametrization proposed in the semiclassical theory of lightly doped antiferromagnets by Shraiman and Siggia.⁵⁶ As discussed in previous work^{24,25}, in the non-SDW phase with $\langle z_\alpha \rangle = 0$, the parameterization in Eq. (2.2) and the coupling in Eq. (A3) lead to electron spectral functions which are not centered at \mathbf{K}_v ; once Néel order has been disrupted, there is no special reason for the electronic spectrum to be pinned at the magnetic Brillouin zone boundary. The computed²⁴ electron spectral functions have a “Fermi arc” structure, similar to those observed experimentally. An additional mechanism for Fermi arc behavior is from the phase fluctuations of the superconducting order, and these effects will appear in our theory from the “Josephson” term introduced in Eq. (2.11) between the $f_{\pm p}$ fermions and the pairs formed out the states near \mathbf{Q}_a ; a recent work⁵⁷ has examined classical thermal phase fluctuations present at high temperatures, and our formulation allows for a systematic consideration of quantum phase fluctuations at low temperatures.

Indeed, our primary focus here is on the electronic excitations near the \mathbf{Q}_a wavevectors. For these we need electromagnetic charge $-e$ “doublon” annihilation operators g_q , where $q = \pm$. The g_\pm will be the central actors in our analysis. Note that the g_q do not carry any valley index, and the two charges of g_\pm specify all the fermionic degrees of freedom at all the \mathbf{Q}_a in Fig. 1. The g_\pm are related to the physical electrons by Eq. (2.1) and²⁶

$$\begin{pmatrix} G_{1\uparrow} \\ G_{1\downarrow} \end{pmatrix} = \mathcal{R}_z \begin{pmatrix} -g_- \\ -g_+ \end{pmatrix} \quad , \quad \begin{pmatrix} G_{2\uparrow} \\ G_{2\downarrow} \end{pmatrix} = \mathcal{R}_z \begin{pmatrix} g_- \\ -g_+ \end{pmatrix}, \quad (2.4)$$

where the SU(2) rotation \mathcal{R}_z was defined in Eq. (2.3). In the SDW state, the \pm indices of the g_\pm fermions (and also of the $f_{\pm p}$ fermions) become equivalent to the \uparrow, \downarrow spin indices quantized along the direction of the Néel order *i.e.* the g_\pm are conventional electron opera-

tors.²⁴ However, in the phase with spin rotation invariance preserved, \pm gauge charges can be interpreted as sublattice indices which determine the sublattice on which the fermion is predominantly (but not exclusively) located.

We will carry out our analysis in the framework of an effective field theory for the g_{\pm} coupled to the A_{μ} emergent gauge field. The complete Lagrangian for our field theory has the following structure (field theories for bosonic spinons and spinless fermions were also considered in early work^{58,59,60,61}):

$$\begin{aligned}
\mathcal{L} &= \mathcal{L}_g + \mathcal{L}_z + \mathcal{L}_f + \mathcal{L}_{fg} + \mathcal{L}_{zf} + \mathcal{L}_{zg} + \mathcal{L}_A \\
\mathcal{L}_g &= g_+^{\dagger} \left[(\partial_{\tau} - iA_{\tau} + iea_{\tau}) - \frac{1}{2m^*} (\nabla - i\mathbf{A})^2 - \mu \right] g_+ \\
&+ g_-^{\dagger} \left[(\partial_{\tau} + iA_{\tau} + iea_{\tau}) - \frac{1}{2m^*} (\nabla + i\mathbf{A})^2 - \mu \right] g_- \\
&- \lambda g_+^{\dagger} g_-^{\dagger} g_- g_+ .
\end{aligned} \tag{2.5}$$

We have only written out explicitly the Lagrangian \mathcal{L}_g which involves the g_{\pm} fermions, and which will be the basis for almost all the computations in the body of this paper. The term \mathcal{L}_{fg} coupling the $f_{\pm p}$ and g_{\pm} fermions will be described below; all other terms have been discussed previously^{24,26} and are recalled in Appendix A. In Eq. (2.5), a_{τ} is the external electrostatic potential whose coupling shows that both g_{\pm} carry charge $-e$. The fluctuations of a_{τ} are controlled by the action

$$\mathcal{S}_a = \frac{1}{4\pi} \int d\tau \int \frac{d^2k}{4\pi^2} |\mathbf{k}| |a_{\tau}(\mathbf{k}, \tau)|^2, \tag{2.6}$$

which leads to the Coulombic repulsion e^2/r between all the g_{\pm} particles. The magnetic dipole interactions associated with fluctuations of the electromagnetic vector potential \mathbf{a} can be safely ignored. The g_{\pm} carriers have any effective mass m^* , and experience a chemical potential μ .

A. Fermion pairings

1. g_{\pm} pairing

We will be especially interested in the pairing of the g_{\pm} fermions as described by \mathcal{L}_g . Indeed, we will present arguments below in favor of the proposition that an s -wave pairing of the g_{\pm} is the primary pairing instability of the underdoped cuprates: the pairing of the $f_{\pm p}$ fermions, and of the physical electrons Ψ_{α} will be shown to follow from it.

Eq. (2.5) already includes an attractive contact BCS interaction, λ , between the g_{\pm} . This attraction is permitted by the underlying symmetries,²⁶ and so can be written down on phenomenological grounds. More physically, the longitudinal component of the A_{μ} gauge force

provides an important component of the attractive force between the g_+ and g_- fermions: this is simply the attractive ‘‘Coulomb’’ force between two opposite charges. This will be Thomas-Fermi screened by the compressible fermion state to an attractive force with a range of order the Fermi wavelength. It is clear that this force prefers an s -wave pairing between the g_{\pm} fermions. An additional contribution to the s -wave attractive force comes from the term \mathcal{L}_{zg} in Eq. (A5). Integrating out the z_{α} spinons, we find a contact attractive interaction $\sim -\lambda_{zg}^2$.

However, the key source of the s -wave pairing of the g_{\pm} is the force associated with the *transverse* components of the A_{μ} gauge field. As long as we are in the phase without SDW order, these remain long-range and unscreened. The nature of the A_{μ} fluctuations are similar to those of the fermionic U(1) spin liquid⁶² or the Halperin-Lee-Read state.⁶³ We have the following propagator for the transverse part of the gauge field:

$$\langle A_i(\mathbf{q}, \omega) A_j(-\mathbf{q}, -\omega,) \rangle = \left[\delta_{ij} - \frac{q_i q_j}{q^2} \right] \frac{1}{\chi q^2 + \gamma |\omega|/q + \Delta_{\text{AF}}}. \quad (2.7)$$

In our case, the effective gauge-field propagator contains contributions both from the z_{α} spinons and from the charge carrying fermions $f_{\pm p}$, g_{\pm} . The spinon contributions to the susceptibility χ from Eq. (A1) were discussed in Ref. 64. The fermions yield $\chi = [6\pi^2\nu]^{-1}$, with the effective density of states, $\nu = \bar{\mu}/\pi$, determined by the reduced mass of the holons and doublons, $\bar{\mu} = m^* m_f / (2m^* + m_f)$ (here m_f is related to the masses in Eq. (A2), and the factors of 2 arise from the valley degeneracy). The damping term γ comes from the Landau damping of fermions and is given by the sum of two Fermi-momenta $\gamma = (p_{\text{F}}^{(g)} + 2p_{\text{F}}^{(f)}) / (2\pi)$. Finally, the ‘‘mass’’ term Δ_{AF} arises from the Higgs mechanism in the state with SDW order with

$$\Delta_{\text{AF}} \sim |\langle z_{\alpha} \rangle|^2, \quad (2.8)$$

as discussed in Appendix A.

Pairing due to transverse gauge forces has been considered previously in the context of spin liquids. Because the magnetic force between two oppositely directed currents is repulsive, a pairing between fermions could occur only in unusual channels,^{65,66} in particular in the ‘‘Amperian’’ channel where the fermions on the same side of the Fermi surface pair up.⁶⁶ However, in our case note that the g_+ and g_- carry opposite A_{μ} gauge charges, and so the magnetic force is *attractive* in the traditional s -wave BCS channel of pairing between fermions on opposite sides of the Fermi surface. Indeed, this problem of pairing by transverse gauge forces between Fermi surfaces of opposite charges has been considered previously by Bonesteel, McDonald, and Nayak,⁶⁷ and by Ussishkin and Stern⁶⁸ in the context of double layer quantum Hall systems each at filling fraction $\nu = 1/2$. In this quantum Hall problem, the electrons in the two layers have opposite gauge charges with respect to an ‘‘antisymmetric’’ U(1) gauge field whose flux measures out-of-phase density fluctuations in the two layers, and their s -wave BCS instability leads to a paired quantum Hall state. An

Eliashberg analysis of such a pairing instability due to transverse gauge forces was carried out in these works,^{67,68} and their results can be related to our problem. An important result obtained in these studies was that while the low-energy gauge fluctuations lead to very singular electron self-energies in the normal state (including non-Fermi liquid behavior), they are not^{69,70} pair-breaking; the pairing instability remains very strong. This should be contrasted with the behavior near ferromagnetic quantum critical points, where there is a similar anomalous self-energy in the normal state, but the ferromagnetic fluctuations are pair-breaking to p -wave superconductivity.^{70,71,72} For our problem, the estimate of the s -wave pairing temperature is $T_{p0} \sim \gamma^2/(m^*3\chi^2)$. Using the values of χ and γ quoted below Eq. (2.7), and ignoring the spinon contribution to χ , we arrive at the simple estimate $T_{p0} \sim E_F$, where $E_F = p_F^2/(2m^*)$ is the Fermi energy for electrons. To the extent we can work within the context of \mathcal{L}_g in Eq. (2.5), we can understand this estimate on dimensional grounds. Note that in the non-magnetic phase, the only dimensional parameters appearing in Eq. (2.7) are associated with the Fermi surface, and there is no arbitrary coupling constant in the coupling between g_{\pm} and A_{μ} . In this respect, this problem is similar to the three-dimensional Fermi gas at a Feshbach resonance. Consequently, the mean-field pairing temperature T_{p0} can only be of order the available energy scale, which are the Fermi energies. In reality, the actual value of T_{p0} will be also influenced by the spinon contribution to χ , the Coulomb repulsion e^2/r between the g_{\pm} , the contribution of the $f_{\pm p}$ to the A_{μ} polarization, and the value of λ .

Given the quenching of the transverse gauge propagator in Eq. (2.7) in the phase with $\langle z_{\alpha} \rangle \neq 0$, we can expect that the pairing instability will become weaker in the SDW ordered state. This then sets up a natural and appealing mechanism for the suppression of T_{p0} after the onset of SDW order. Indeed, it offers a basis for the theory of “competing orders”³⁴ which has many attractive phenomenological features.

We have now established that \mathcal{L}_g has a strong pairing instability to a state where

$$\langle g_+(\mathbf{k})g_-(-\mathbf{k}) \rangle = \Delta_g, \quad (2.9)$$

where we can take the pairing amplitude Δ_g to be independent of \mathbf{k} near the Fermi level. Then, what is the pairing amplitude for the physical electron operators in Eq. (2.1)? We assume, for simplicity, that we are in a non-magnetic state where $\langle z_{\alpha}^* z_{\beta} \rangle \sim \delta_{\alpha\beta}$. Then from Eq. (2.4) we obtain

$$\begin{aligned} \langle G_{1\alpha}(\mathbf{k})G_{1\beta}(-\mathbf{k}) \rangle &= -\langle G_{2\alpha}(\mathbf{k})G_{2\beta}(-\mathbf{k}) \rangle \sim \varepsilon_{\alpha\beta}\Delta_g; \\ \langle G_{1\alpha}(\mathbf{k})G_{2\beta}(-\mathbf{k}) \rangle &= 0. \end{aligned} \quad (2.10)$$

Comparing with Fig. 1, we see that this is precisely the pairing signature expected for d -wave pairing of the electrons; see also Fig. 4.

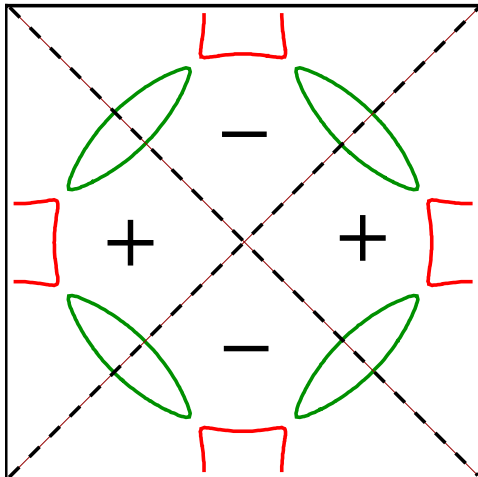


FIG. 4: Sign of the d -wave pairing amplitude superimposed on the electron and hole pockets of the SDW metal. Note that these signs correspond to s -wave pairing of the electron pockets and p -wave pairing of the hole pockets, as explained in the text.

2. $f_{\pm p}$ pairing

Finally, we turn to the pairing of the $f_{\pm p}$ fermions. Just as was the case for the g_{\pm} fermions, the A_{μ} gauge forces will prefer a s wave pairing of oppositely charged $f_{\pm p}$ fermions. However, there is a competing “proximity” effect arising from the paired g_{\pm} fermions. This proximity effect is due to a Josephson coupling between g_{\pm} and $f_{\pm p}$ pairs. The form of such a Josephson term is tightly constrained by the projective symmetry group (PSG), which was presented in detail in Refs. 24,26 and the transformations needed here are listed in Table I. An analysis based on Table I shows that the simplest allowed coupling between the g_{\pm} and $f_{\pm p}$ pairs which is invariant under the PSG is

$$\mathcal{L}_{fg} = -iJ_{fg} [g_+g_-] \left[f_{+1} \vec{D}_x f_{-1} - f_{+1} \vec{D}_y f_{-1} + f_{+2} \vec{D}_x f_{-2} + f_{+2} \vec{D}_y f_{-2} \right] + \text{H.c.}, \quad (2.11)$$

where J_{fg} is the Josephson coupling, $D_i \equiv \partial_i - qA_i$ is the co-variant derivative acting on a field with charge q , and $a \vec{D}_i b \equiv aD_ib - (D_ia)b$. Note that Table I does not permit any term without a spatial gradient. From the structure of the Josephson coupling in Eq. (2.11) we see that the proximity effect induces a p -wave pairing of the $f_{\pm p}$ fermions. Thus there is *frustration* in the $f_{\pm p}$ pairing, with the A_{μ} gauge forces preferring s -wave.

At the microscopic level, a computation of the pairing of the $f_{\pm p}$ fermions in the SDW ordered state has been carried out by Sushkov and collaborators.^{74,75,76,77} They showed that, for a suitable range of parameters, the long-range spin-wave interaction preferred a p -wave pairing. In our formulation this long-range attraction between the $f_{\pm p}$ is mediated by the Shraiman-Siggia term in Eq. (A3). Note that this Shraiman-Siggia term does not apply to the g_{\pm} , and so the corresponding interaction is absent there.

On the basis of our arguments above, and the complementary microscopic

	T_x	$R_{\pi/2}^{\text{dual}}$	I_x^{dual}
g_+g_-	g_+g_-	$-g_+g_-$	g_+g_-
$f_{+1}f_{-1}$	$-f_{+1}f_{-1}$	$f_{+2}f_{-2}$	$f_{+2}f_{-2}$
$f_{+2}f_{-2}$	$-f_{+2}f_{-2}$	$-f_{+1}f_{-1}$	$f_{+1}f_{-1}$
$f_{+1} \overleftrightarrow{D}_x f_{-1}$	$f_{+1} \overleftrightarrow{D}_x f_{-1}$	$-f_{+2} \overleftrightarrow{D}_y f_{-2}$	$f_{+2} \overleftrightarrow{D}_x f_{-2}$
$f_{+1} \overleftrightarrow{D}_y f_{-1}$	$f_{+1} \overleftrightarrow{D}_y f_{-1}$	$f_{+2} \overleftrightarrow{D}_x f_{-2}$	$-f_{+2} \overleftrightarrow{D}_y f_{-2}$
$f_{+2} \overleftrightarrow{D}_x f_{-2}$	$f_{+2} \overleftrightarrow{D}_x f_{-2}$	$f_{+1} \overleftrightarrow{D}_y f_{-1}$	$f_{+1} \overleftrightarrow{D}_x f_{-1}$
$f_{+2} \overleftrightarrow{D}_y f_{-2}$	$f_{+2} \overleftrightarrow{D}_y f_{-2}$	$-f_{+1} \overleftrightarrow{D}_x f_{-1}$	$-f_{+1} \overleftrightarrow{D}_y f_{-1}$

TABLE I: PSG transformations deduced from the PSG of the $f_{\pm q}$ in Table II in Ref. 24, the PSG of the g_{\pm} in Table III in Ref. 26, and the PSG of \mathbf{A} in Eq. (12) of Ref. 73. The transformations are T_x : translation by one lattice spacing along the x direction; $R_{\pi/2}^{\text{dual}}$: 90° rotation about a dual lattice site on the plaquette center ($x \rightarrow y, y \rightarrow -x$); I_x^{dual} : reflection about the dual lattice y axis ($x \rightarrow -x, y \rightarrow y$).

computations^{74,75,76,77}, we conclude that the s -wave pairing of the g_{\pm} fermions is the dominant instability, and the Josephson coupling in Eq. (2.11) induces a sympathetic p -wave pairing of the $f_{\pm p}$ fermions. A key point is that the A_μ gauge forces will be pair-breaking towards this p -wave pairing,^{70,71,72} and consequently the $f_{\pm p}$ pairing amplitude will be quite weak.

Specifically, combining Eqs. (2.11) and (2.9), we deduce that the proximity-effect pairing of the $f_{\pm p}$ fermions induced by the g_{\pm} fermions has the p -wave form

$$\begin{aligned}
\langle f_{+1}(\mathbf{k})f_{-1}(-\mathbf{k}) \rangle &\sim (k_x - k_y)J_{fg}\Delta_g; \\
\langle f_{+2}(\mathbf{k})f_{-2}(-\mathbf{k}) \rangle &\sim (k_x + k_y)J_{fg}\Delta_g; \\
\langle f_{+1}(\mathbf{k})f_{-2}(-\mathbf{k}) \rangle &= 0,
\end{aligned} \tag{2.12}$$

where the momentum dependencies are a consequence of the spatial gradients in Eq. (2.11), and the pairing amplitudes between fermions with like A_μ charges are zero. Finally, from these results and Eq. (2.2), we can deduce the pairing of the physical electron operators in $F_{v\alpha}$ in Eq. (2.1):

$$\begin{aligned}
\langle F_{1\alpha}(\mathbf{k})F_{3\beta}(-\mathbf{k}) \rangle &\sim \varepsilon_{\alpha\beta}(k_x - k_y)J_{fg}\Delta_g; \\
\langle F_{2\alpha}(\mathbf{k})F_{4\beta}(-\mathbf{k}) \rangle &\sim \varepsilon_{\alpha\beta}(k_x + k_y)J_{fg}\Delta_g
\end{aligned} \tag{2.13}$$

and all other $F_{v\alpha}$ pairings vanish. A glance at Figs. 1 and 4 shows that these are precisely the pairings associated with a d -wave pairing signature of the physical Ψ_α electrons. The

momentum dependencies in Eq. (2.13) shows that the pairing amplitude changes sign across the Brillouin zone diagonals. Also, the vanishing of the pairing along these zone diagonals shows that there will be gapless “nodal” fermionic excitations.

We close this section by noting that the structure of the Josephson coupling in Eq. (2.11) is closely connected to that appearing in the model of Geshkenbein, Ioffe and Larkin.¹⁷ They considered a phenomenological model of charge $-2e$ bosons, representing pairs of electrons near the \mathbf{Q}_a , coupled to fermions near the \mathbf{K}_v . Their boson-fermion Josephson coupling had a matrix element which changed sign along the Brillouin zone diagonals. Identifying their boson b as $b \sim g_+g_-$, we see that Eq. (2.11) also shares these features.

III. QUANTUM OSCILLATIONS IN THE NORMAL STATE

This section will consider the low temperature transport properties of the paired state of the g_{\pm} described by \mathcal{L}_g which is driven normal by a strong applied magnetic field, H .

We begin by a simple estimate of the depairing field, $H_{p2}(0)$, associated to the pairing temperature, T_{p0} . In the absence of a complete Eliashberg theory of the influence of the transverse gauge fluctuations, we will be satisfied here with an estimate based on the weak-coupling BCS theory result for the upper critical field of a clean two-dimensional superconductor (note that the value of the upper critical field depends on the purity^{78,79} and dimensionality of the system^{80,81}). For the purpose of numerical estimates, we ignore here the quantum oscillation phenomena in the transition point itself, which as discussed below may lead to a reentrant behavior. Within these assumptions, we have the following BCS formula^{78,81} that we associate with the “quantum depairing field” (here, we restore the fundamental physical constants):

$$\frac{eH_{p2}(0)}{m_*c} = \frac{\pi^2 k_B T_{p0}^2}{\gamma_E \hbar T_F}, \quad (3.1)$$

where e is the electron charge, c is the speed of light, m_* is the effective mass of carriers in the pocket, k_B is the Boltzmann constant, $T_F = p_F^2/(2k_B m_*)$ is the Fermi temperature for the electrons in the pocket, p_F is their Fermi momentum, and $\gamma_E = 1.781\dots$ is the exponential of Euler’s constant. The onset of quantum oscillations in the cuprate experiments^{27,28,29,30,31} is identified here with the quantum depairing field, $H_{p2}(0)$. The former is about $H_{p2}(0) \sim 50$ Tesla. The quantum oscillation measurements also provide information for the effective electron mass, which appears to be of order free electron mass or a few times larger (the exact values vary in experiment) and for the area of the electron Fermi surface, which is estimated to be a few percent of the total area of the Brillouin zone, which in turn is determined by the lattice constants for YBCO. This information allows us to extract all necessary parameters.

The Fermi temperature is related to the frequency of quantum oscillations, F_{SdH} , as follows:

$$T_{\text{F}} = \frac{\pi \hbar^2}{k_{\text{B}} m_e \Phi_0} \left(\frac{m_e}{m^*} \right) F_{\text{SdH}}, \quad (3.2)$$

where $\Phi_0 = (2.07 \times 10^{-15}) \text{ T} \cdot \text{m}^2$ is the flux quantum. The first factor in Eq. (3.2) contains only fundamental constants and is equal to $\frac{\pi \hbar^2}{k_{\text{B}} m_e \Phi_0} = 1.33 \text{ K/T}$ (K and T correspond to the units of Kelvin and Tesla respectively). Using Eq. (3.1), we can write the following relation between the pairing temperature and the quantum pairing field and the Fermi temperature:

$$T_{\text{p0}} = \sqrt{\frac{\gamma_{\text{E}} \mu_{\text{B}}}{\pi^2 k_{\text{B}}} \left(\frac{2m_e}{m^*} \right) T_{\text{F}} H_{\text{p2}}(0)}, \quad (3.3)$$

where $\mu_{\text{B}} = e\hbar/(2|e|c)$ is the Bohr's magneton. Converting all quantities to the units of Tesla and Kelvin relevant to the interpretation of experimental data and using the actual values of the corresponding physical constants, we can express the Fermi temperature for the electrons in the pocket and the corresponding pairing temperature as follows

$$T_{\text{F}} \text{ K} \approx \left(\frac{1.33m_e}{m^*} \right) [F_{\text{SdH}} \text{ T}] \quad (3.4)$$

and

$$T_{\text{p0}} \text{ K} \approx \sqrt{\frac{0.24m_e}{m^*} [T_{\text{F}} \text{ K}][H_{\text{p2}}(0) \text{ T}]}, \quad (3.5)$$

where $[T_{\text{F}} \text{ K}]$ is the Fermi temperature expressed in Kelvin, and $[H_{\text{p2}}(0) \text{ T}]$ and $[F_{\text{SdH}} \text{ T}]$ are the quantum critical field and the period of the Shubnikov-de Haas oscillations expressed in Tesla. We emphasize that the above estimates assume the applicability of the weak-coupling BCS theory and a circular Fermi surface for the electron pocket. Therefore, Eqs. (3.1 – 3.5) are not expected to determine exactly the numerical coefficients, but should provide correct order-of-magnitude estimates. Using the available experimental data, *e.g.* from Ref. [27], which estimates the period of oscillations to be $F_{\text{SdH}} \sim 530 \text{ T}$ and onset of oscillations (the critical pairing field in our theory) as $H_{\text{p2}}(0) \sim 50 \text{ T}$, we get the following relation between the zero-field pairing temperature and the Fermi temperature: $T_{\text{p0}} [\text{K}] \approx \sqrt{m_e/m^*} \sqrt{12 [\text{K}][T_{\text{F}} \text{ K}]}$ and $T_{\text{F}} \approx (m_e/m^*) 700 \text{ K}$. Finally, the estimates for the actual numerical values of T_{F} and T_{p0} depend on the effective mass for electrons. Various experiments report different values for the latter, $m^* \sim (1 - 3)m_e$. As explained below in Secs. III B and III C, one should be careful in extracting the effective mass from the temperature dependence of the oscillations in this phase, because there may be other effects due to superconducting and gauge fluctuations, which will change the temperature dependence of the amplitude in the Lifshitz-Kosevich formula. In addition, if the Fermi surface and/or the quasiparticle weight factor are anisotropic, it would also modify the effective temperature dependence in the Lifshitz-Kosevich formula⁸² In particular, if the

anisotropy of the quasiparticle renormalization Z -factor, $Z_{\mathbf{p}}$, is not taken into account, the effective mass extracted from the quantum oscillation measurements will overestimate the actual effective mass by the factor of $\langle 1/Z_{\mathbf{p}} \rangle_{\text{FS}}$,⁸² where the angular brackets imply averaging over the Fermi surface. However, if we now assume that the effective mass for the electronic excitations in the pocket is of order free electron mass (as suggested by experiments), $m^* \sim m_e$, then we get the Fermi temperature of the electron pocket $T_F \approx 700$ K, the pairing temperature $T_{p0} \approx 100$ K, and the zero-temperature BCS superconducting gap, $\Delta/k_B = (\pi/\gamma_E) T_{p0} \approx 200$ K.

The relatively large ratio between the electron pairing temperature and the Fermi temperature (T_{p0}/T_F) $\sim (1/7)$ justifies our earlier conclusion about strong Cooper pairing in the electron pocket. We note further that a complete description of the finite temperature pseudogap region likely requires the inclusion of further interactions between the Cooper pairs. A particularly interesting possibility appears within an effective model where the paired electrons in the pockets interact on the lattice. This type of model for the electron pairs, $\langle g_+ g_- \rangle$, may have a superconductor-to-insulator phase transition with a Mott-type gap of order, J , accompanied by development of charge order associated with the density of bosons⁴³ and the monopole Berry phases^{73,83} in \mathcal{L}_A (see Appendix A 4).

In the following, we will describe the Shubnikov-de Haas oscillations in the resistivity at $H > H_{p2}(T)$. For reference, we recall the Lifshitz-Kosevich formula for the oscillatory component of the resistivity ρ (retaining only the lowest oscillation harmonic)

$$\frac{\rho_{\text{osc}}(H)}{\rho_{\parallel}(H=0)} = \frac{X(T)}{\sinh[X(T)]} \exp\left(-\frac{\pi}{\omega_c \tau}\right) \cos\left(\frac{2\pi E_F}{\omega_c}\right), \quad (3.6)$$

where $\rho_{\parallel}(H=0)$ is the Drude resistivity in zero field, $X(T) = 2\pi^2 T/\omega_c$, τ is the elastic scattering time from impurities, $\omega_c = eH/(m^*c)$ is the cyclotron frequency.

We begin our analysis of transport by discussing the fate of the Ioffe-Larkin composition rule in our system in Section III A. In Section III B, we will describe the corrections to the Lifshitz-Kosevich result from the fluctuations of the A_{μ} gauge field, while the influence of pairing fluctuations will be discussed in Section III C.

A. Ioffe-Larkin composition rule

Before turning to the computation of the transport properties at $H > H_{p2}(T)$ in the subsections below, we need to discuss an important, but technical, issue. In previous studies of spin-charge separation in the cuprates, a crucial ingredient in the computation of the physical conductivity was the Ioffe-Larkin composition rule.^{62,84} This states the resistivities of the spinons and charge carriers add to yield the physical resistivity. In our present situation, there is a crucial difference from the models considered in these works: our g_{\pm} fermions carry opposite charges under the internal A_{μ} gauge field, and the same charge under

the electromagnetic gauge field a_μ . In contrast, the previous theories had holons carrying only a single charge under the analog of A_μ . An immediate consequence for our theory is that the cross-polarization operator between the two gauge fields, Π_{Aa} , vanishes identically: the g_+ and g_- fermions induce opposite polarizations which cancel each other. (More formally, this can be seen by the PSG of the \mathbf{A} gauge field⁷³, which changes sign under translation by a lattice site, and so cannot couple linearly to \mathbf{a} at long wavelengths.) In other words, in the presence of an applied electromagnetic field a_μ , the physical current is carried equally by the g_+ and the g_- . In this current carrying state, the A_μ currents of the g_+ and g_- travel in opposite directions, leading to no net internal gauge current; consequently, there is also no spinon current. The final conclusion is then very simple: the physical conductivity is just the sum of the conductivities of the g_+ and g_- , and the traditional Ioffe-Larkin rule does not apply to our model.

B. Gauge field fluctuations

The influence of gauge fluctuations on magnetotransport was examined in the context of the $\nu = 1/2$ quantum Hall state,^{85,86} and here we will adapt these earlier results to our problem. This analysis was carried out using the quasiclassical method, in which the gauge field fluctuations are treated as a random static “magnetic” field which influences the cyclotron motion of the fermions. We will follow the same method here.

There are two potential sources of the random field. In the quantum Hall case, the most important source was the local field induced by the Chern-Simons term from the impurity potential. This source is absent in our case, as we do not have a Chern-Simons term. Indeed, the PSG of the \mathbf{A} field⁷³ shows that only impurities which locally break time-reversal can induce a non-zero flux of \mathbf{A} ; we will assume that such impurities are absent. An important consequence is that the amplitude of the SdH oscillations in Eq. (3.6) remains unaffected at $T = 0$ by the presence of the gauge field.

The second source of the random field was the thermal fluctuations of \mathbf{A} . For a random field, $h = \nabla \times \mathbf{A}$, with equal time correlations given by

$$\langle h(\mathbf{r})h(\mathbf{r}') \rangle = U(|\mathbf{r} - \mathbf{r}'|), \quad (3.7)$$

Mirlin *et al.*⁸⁶ showed that the SdH oscillations in Eq. (3.6) are suppressed by a factor $\exp(-S_h)$ where

$$S_h = \pi R_c^2 \int_0^\infty \frac{dq}{q} J_1^2(qR_c) \tilde{U}(q). \quad (3.8)$$

Here $R_c = \sqrt{2E_F/m^*}/\omega_c$ is the cyclotron radius of fermions at the Fermi level, and $\tilde{U}(\mathbf{q})$ is the Fourier transform of $U(\mathbf{r})$. In the quasiclassical limit, the equal-time gauge field

correlations can be evaluated from Eq. (2.7) to yield

$$\tilde{U}(q) = \frac{Tq^2}{\chi q^2 + \Delta_{\text{AF}}}. \quad (3.9)$$

We can also deduce from Eq. (2.7) a necessary condition for the applicability of the quasiclassical approximation: the characteristic frequency $\omega \sim (q/\gamma)(\chi q^2 + \Delta_{\text{AF}})$ at the characteristic wave-vector $q \sim 1/R_c$ should be smaller than T . Now, we can insert Eq. (3.9) into Eq. (3.8) and obtain

$$S_h = \frac{\pi R_c^2 T}{\chi} I_1 \left(R_c \sqrt{\Delta_{\text{AF}}/\chi} \right) K_1 \left(R_c \sqrt{\Delta_{\text{AF}}/\chi} \right), \quad (3.10)$$

where I_1 and K_1 are modified Bessel functions. In the phase without SDW order, where $\Delta_{\text{AF}} = 0$, we then have

$$S_h = \frac{\pi E_F T}{m^* \chi \omega_c^2}. \quad (3.11)$$

The value of S_h decreases monotonically into the phase with SDW order *i.e.* the SdH oscillations have a larger amplitude in the SDW state. Deep in the SDW state, where $\Delta_{\text{AF}} \gg \chi/R_c^2$, we have the limiting result for S_h (which is always smaller than the value of S_h in Eq. (3.11))

$$S_h = \frac{\pi T}{\omega_c} \sqrt{\frac{E_F}{2m^* \chi \Delta_{\text{AF}}}}. \quad (3.12)$$

The thermal suppression of the SdH oscillations in Eqs. (3.10-3.12) by the factor $\exp(-S_h)$ will combine with the factor $\exp(-2\pi^2 T/\omega_c)$ already present in Eq. (3.6). While the T dependencies in the two factors are the same, they are distinguished by their B dependencies. In particular, we have $S_h \sim T/B^2$ in Eq. (3.11), and this can serve as a characteristic signature of gauge field fluctuations in an algebraic charge liquid.

C. Pairing fluctuations

This subsection will describe the corrections to Eq. (3.6) in the context of a traditional fluctuating superconductivity computation built on BCS theory. We will not examine the interesting question of how the transverse A_μ fluctuations will modify the Cooperon operator. However, given the absence of pair-breaking effects in the Eliashberg computation,^{67,68} it is reasonable to expect that the Cooperon will remain the same near the pair-breaking transition. In any case, we can also appeal to the onset of SDW order, which leads to $\Delta_{\text{AF}} > 0$, to quench the gauge fluctuations.

We begin with the Cooperon operator in the quasiclassical approximation as follows

$$C(\varepsilon, \omega; \mathbf{r}, \mathbf{r}') = \mathcal{G}_{\varepsilon+\omega}(\mathbf{r} - \mathbf{r}') \mathcal{G}_{-\varepsilon}(\mathbf{r} - \mathbf{r}') \exp \left[-2ie \int_{\mathbf{r}}^{\mathbf{r}'} \mathbf{a} \cdot d\mathbf{l} \right], \quad (3.13)$$

where $\mathcal{G}_\varepsilon(\rho)$ is the fermion Green's function in the absence of a magnetic field, and the latter (real magnetic field), $\mathbf{H} = \nabla \times \mathbf{a}$, is accounted for only in the gauge factor. Note that in our model, the \pm -electrons carry opposite $e_* = \pm 1$ charges with respect to the “internal” gauge field, \mathbf{A} , but have the same (negative) electron charge, $-e$, with respect to the external electromagnetic field. Hence, we can take advantage of the old results of Helfand and Werthamer,⁷⁸ who have proven that the Cooperon operator, $\hat{C}(\varepsilon, \omega)$, whose kernel is defined via Eq. (3.13), is a diagonal operator in the Landau basis. Its matrix elements are defined simply by the expression without magnetic field, $C_n = \langle n | (\varepsilon, \omega; \mathbf{q} \rightarrow \hat{\boldsymbol{\pi}}) | n \rangle$, but with the momentum \mathbf{q} replaced with the operator of the kinetic momentum of a Cooper pair $\hat{\boldsymbol{\pi}} = [\mathbf{q} - 2ie\mathbf{a}(\hat{\mathbf{r}})]$. The corresponding matrix elements are known from the Landau problem in the elementary single-particle quantum mechanics, *e.g.*, $\langle n | \hat{\boldsymbol{\pi}}^2 | n \rangle = 4eH(n + 1/2)$ (note that the Cooper pair charge is $-2e$ and mass is $2m^*$). The general expression for the Cooperon without a magnetic field is as follows:

$$C(\varepsilon, \omega; \mathbf{q}) = 2\pi\nu \frac{\theta[\varepsilon(\varepsilon - \omega)]}{\sqrt{(2\varepsilon - \omega + (1/\tau)\text{sgn } \varepsilon)^2 + v_F^2 q^2}}, \quad (3.14)$$

where ν is the density of states at the Fermi level and τ is the scattering time. Since we are interested in explaining the quantum oscillations, we assume that the latter is large and set it to $\tau = \infty$. Note that the clean case is in fact more complicated than the disordered limit, because the Green's functions and the Cooperon are non-local objects (*i.e.*, there is no exponential decay in space). The fluctuation propagator for superconducting fluctuations is an operator given by

$$\hat{\mathcal{L}}(\omega) = \left[\lambda_{\text{eff}}^{-1} - T \sum_{\varepsilon} \hat{C}(\varepsilon, \omega) \right]^{-1}. \quad (3.15)$$

For the purpose of describing quantum oscillations, we are interested only in the quantum critical point, $H_{p2}(0)$, which is determined by the divergence of the matrix element at the lowest Landau level of the operator, $\bar{\mathcal{L}}_0(0) = \infty$. This leads to the expression near the quantum pairing field as follows (here and below, the index “0” corresponds to the matrix element at the lowest Landau level):

$$\bar{\mathcal{L}}_0(\omega) = -\frac{1}{\nu} \left[r + \sqrt{\frac{\gamma}{\pi} \frac{|\omega|}{T_{p0}}} \right]^{-1}, \quad (3.16)$$

where $r = [H - H_{p2}(0)]/H$ is the proximity to the pairing transition, and the value of the critical field was specified in Eq. (3.1).

In the expressions so far, the Cooperon dependence on the magnetic field is accounted for only via the gauge factor (3.13). Physically this corresponds to an approximation in which the motion of the Cooper pair in the magnetic field is quantized (more precisely, the center-of-mass motion is quantized), but the cyclotron motion of individual electrons within

a Cooper pair is not accounted for. This quasiclassical approximation is valid if either temperature is relatively large, $T \gg \omega_c$ (note that near $H_{p2}(0)$, $\omega_{p2}/T_{p0} \sim T_{p0}/E_F$, which is small in the conventional weak-coupling BCS theory), or if disorder is strong enough, $\omega_c\tau \ll 1$. In the regime, where the oscillations are observed neither of these conditions is satisfied and therefore one has to take into account Landau quantization of electrons within a Cooper pair. This problem was considered back in the sixties, *e.g.*, by Gruenberg and Günter,⁸⁷ and we reiterate here the main steps to derive the oscillating transition point and the fluctuation effects in its vicinity. The quantity of interest is the fluctuation propagator, which we write as:

$$\mathcal{L}_0(\omega) = \frac{1}{\overline{\mathcal{L}}_0(\omega) - C_{\text{osc}}}, \quad (3.17)$$

where $\overline{\mathcal{L}}_0(\omega)$ is the fluctuation propagator given by Eq. (3.16), which does not take into account oscillations, and C_{osc} is the correction to the Cooperon with the quantum oscillation effects, given by

$$C_{\text{osc}} = \int e^{-eHr^2/4} C(\mathbf{r}) d^2r - \overline{C}_0, \quad (3.18)$$

with \overline{C}_0 is the matrix element for the Cooperon at the lowest Landau level without oscillations and $C(\mathbf{r}) = T \sum_{\varepsilon} \mathcal{G}(\varepsilon, \mathbf{r}; B) \mathcal{G}(-\varepsilon, \mathbf{r}; B)$ and the electron Green's function in a magnetic field is given by

$$\mathcal{G}(\varepsilon, \mathbf{r}; B) = \nu_{\text{mag}} \omega_c \sum_{n_e=1}^{\infty} \frac{e^{-eHr^2/4} L_{n_e}(eHr^2/2)}{i\varepsilon - \omega_c(n_e + 1/2) - \mu + i \text{sgn}(\varepsilon)/(2\tau)}, \quad (3.19)$$

with $L_{n_e}(z)$ being the Laguerre polynomial at the n_e -th *single-electron* Landau level. It is these electron Landau levels that may generate de Haas oscillations above and even within the superconducting phase. The quantity C_{osc} has been considered previously by Mineev⁸⁸ and also by Larkin and one of the authors,⁸¹ and it has the following form (again, we retain only the leading oscillation term, and drop all the higher-order harmonics)

$$C_{\text{osc}}(H) = \frac{4\nu}{3\sqrt{\pi}} \sqrt{\frac{\omega_c}{E_F}} \frac{3X(T)}{\sinh[3X(T)]} \exp\left(-\frac{3\pi}{\omega_c\tau}\right) \cos\left(\frac{2\pi E_F}{\omega_c}\right), \quad (3.20)$$

where $X(T) = 2\pi^2 T/\omega_c$ and $\pi/(\omega_c\tau)$ are the familiar terms, which describe the suppression of quantum oscillations by the temperature and disorder (Dingle factor) correspondingly. Note however that there is an additional factor of 3 in these suppression terms in the leading oscillation harmonics for the Cooperon. This additional suppression (first pointed out by Mineev^{88,89}) is due to the fact that to resolve quantum oscillations coming out of a Cooper pair built of two electrons, one has to “resolve” their relative cyclotron motion without breaking the pair.

Using the expression (3.20), we obtain the fluctuation propagators follows

$$\mathcal{L}_0(\omega) = -\frac{1}{\nu} \left[\frac{H - \overline{H}_{p2}(T)}{H} - C_{\text{osc}}/\nu + \sqrt{\frac{\gamma}{\pi} \frac{|\omega|}{T_{p0}}} \right]^{-1}. \quad (3.21)$$

From Eq. (3.21), we see that the oscillatory part in the Cooperon can be interpreted as a correction to the upper critical field, which too may oscillate and therefore pairing may show a re-entrant behavior at low temperatures. Hence in the regime where quantum oscillations are observed, the exact value of the ‘‘upper critical field’’ (even in the sense of the BCS pairing-depairing transition) is strictly-speaking ill-defined because there are many critical fields as long as oscillations are not suppressed.

Another important circumstance has been pointed out by Champel and Mineev,⁸⁹ who argued that even below the mean-field critical field, $\overline{H}_{p2}(T)$, where the system is paired, one may see (de Haas-van Alfvén) oscillations in the gapless superconductivity region, which is determined by the condition $[H_{p2}(0) - H]/H \ll \sqrt{\omega_{p2}/E_F} \ln(\omega_{p2}/E_F)$ in three dimensions and $[H_{p2}(0) - H]/H \ll \sqrt{\omega_{p2}/E_F}$ in strictly two dimensions [here, $\omega_{p2} = eH_{p2}(0)/(m^*c)$]. We note that $\sqrt{\omega_{p2}/E_F}$ is the Ginzburg parameter, which is typically negligibly small in the conventional BCS systems, but is expected to be larger in the cuprates. The numerical estimates (3.1 – 3.5) in the beginning of this section, suggest a very wide fluctuation Ginzburg region for the strongly-paired small electron pocket of our model; *E.g.*, using the experimental data of Ref. [27], we get $\sqrt{\omega_{p2}/E_F} \sim 1/3$ for the electron pocket⁹⁰. We also emphasize that these possible quantum oscillations in the gapless superconductivity region are different from the effect, which may arise from the normal vortex cores well below the critical field. In fact, the latter effect may be significantly suppressed in the strongly paired phase, where the individual vortex cores are not large enough to support a many-body electron state leading to quantum oscillations.

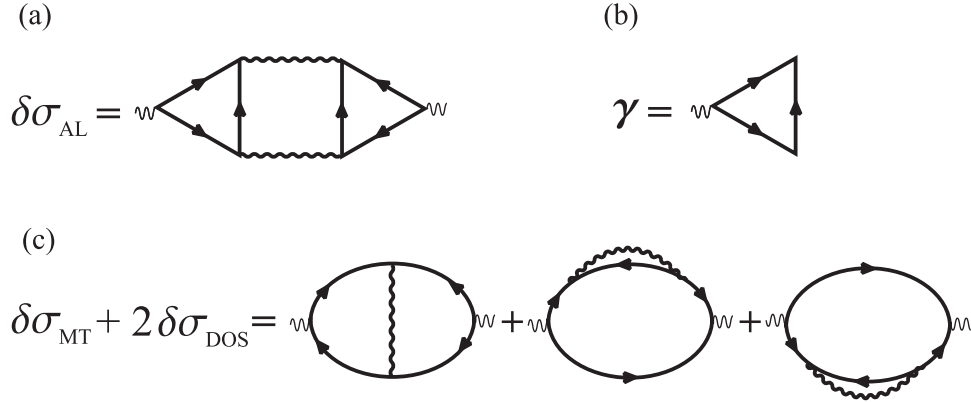


FIG. 5: The relevant diagrams that describe the fluctuation transport near a pairing transition. Fig (1a) shows the Aslamazov-Larkin contribution to conductivity in the clean limit; Fig (1b) shows the current vertex of the Aslamazov-Larkin diagram calculated in Eqs. (3.23) and (3.24); Fig (1c) describes the combined contribution of the Maki-Thompson and density-of-states terms.

We now ready to calculate the fluctuation corrections to the Lifshitz-Kosevich formula in Eq. (3.6). The fluctuation conductivity in the Gaussian approximation is given by the sum of the Aslamazov-Larkin, density-of-states, and Maki-Thompson diagrams⁹¹ (see Fig. 5). In a strong magnetic field and low temperature, all these diagrams are generally of the same order and in a disordered system all play an important role. However, in the super-clean case of $\omega_c\tau \rightarrow \infty$, the Maki-Thompson and density-of-states terms cancel each other exactly at least for the non-oscillating terms^{81,92} and only the Aslamazov-Larkin term⁹³ survives. The longitudinal part of the electromagnetic response tensor has been considered by Larkin and one of the authors⁸¹ and reads

$$Q(\omega) = 8\nu e^2 T \sum_{\Omega} \gamma_{01}^2(\Omega, \omega) \mathcal{L}_0(\Omega) \mathcal{L}_1, \quad (3.22)$$

where $\mathcal{L}_0(\Omega)$ is the Cooper pair propagator at the lowest Landau level given by Eq. (3.21), \mathcal{L}_1 is the Cooper pair propagator at the first Landau level, which near $H_{p2}(0)$ is not singular and can be treated as a constant, and $\gamma_{01}(\Omega, \omega)$ is a matrix element between the first and the lowest Landau level of the current vertex]. The current vertex operator is defined by $\hat{\gamma}(\Omega, \omega) = \gamma(\mathbf{q} \rightarrow \boldsymbol{\pi}; \Omega, \omega)$, where the latter quantity is given by the three-Green's function block:

$$\gamma(\mathbf{q}; \Omega, \omega) = T \sum_{\varepsilon} \int \frac{d^2p}{(2\pi)^2} \mathbf{v} \mathcal{G}_{\varepsilon}(\mathbf{p}) \mathcal{G}_{\varepsilon-\omega}(\mathbf{p}) \mathcal{G}_{\Omega-\varepsilon}(\mathbf{q}-\mathbf{p}). \quad (3.23)$$

The matrix element $\gamma_{01}(\Omega, \omega)$ was calculated in Ref. 81 and reads

$$\gamma_{01}(\Omega, \omega) = -\frac{\nu r_H}{\sqrt{2}} \frac{1}{1+|\omega|\tau} \left[1 - \frac{\sqrt{\pi} r_H}{2} \frac{r_H}{v_F} (|\Omega| + |\Omega - \omega| + |\omega|) \right] + \gamma_{\text{osc}}, \quad (3.24)$$

where $r_H = 1/\sqrt{2eH}$ is the magnetic length for Cooper pairs. Note that in Eq. (3.24), we do not write explicitly the oscillation contribution, γ_{osc} . The oscillations coming from the vertices are expected to have the usual Fermi liquid form, because the two graphs corresponding to the two vertices when “glued together” essentially reproduce the Drude conductivity diagram and therefore their contribution can be estimated modulo a numerical coefficient in the overall amplitude. Using the technique developed in Ref. [81], we find the following main result for the fluctuation conductivity, which includes the leading oscillation terms as well (here, we address only the zero-temperature contribution):

$$\delta\sigma = \frac{e^2}{\pi^2} \left[1 + \eta \frac{\rho_{\text{osc}}(H)}{\rho(0)} \right] \ln \left\{ \frac{1}{[H - \overline{H}_{p2}(0)] / H - C_{\text{osc}}/\nu} \right\}, \quad (3.25)$$

with C_{osc} given explicitly by Eq. (3.20) $\eta \sim 1$ is a positive numerical coefficient, and $\rho_{\text{osc}}(H)/\rho(0)$ is the ratio of the Fermi liquid oscillation term and the Drude resistivity in

Eq. (3.6). The latter does not involve any additional factors in the temperature and Dingle-temperature dependence as opposed to the Cooperon term, which determines oscillations in the transition point itself.⁹⁴ We observe that Eq. (3.25) describes a decrease in the amplitude of the SdH oscillations upon approaching the superconducting pairing instability.

Our result in Eq. (3.25) may have an interesting physical interpretation: The Cooper pair propagator $\mathcal{L}_n(\omega) = 1/\lambda_{\text{eff}} \langle \Delta^*(\omega)\Delta(\omega) \rangle$ corresponds to the density of Cooper pairs at the n -th Landau level with the energy ω (at least at $T = 0$, the Matsubara frequency can be converted into a real frequency via Feynman rotation). Near $H_{p2}(0)$, only the Cooper pairs at the lowest Landau level play a significant role and the total density of such pairs is given by the integral over frequency [*cf.*, Eq. (3.22)]: $N_{\text{cp}} \sim \int d\omega/(2\pi)\mathcal{L}_0(\omega) \propto -\ln \{H/[H - H_{p2}(0)]\}$. Hence, the Cooper pair density scales as a logarithm in the proximity to the magnetic-field-tuned quantum transition and each electron within a fluctuating pair produces an oscillation term. If temperature and Dingle suppression are small, the functional dependence of the oscillatory part of the fluctuation conductivity is dominated by the Cooperon, C_{osc} . The corresponding oscillation term should also survive below the pairing transition in the gapless superconductivity region. We note here that if such a term is detected in experiment, then the application of the usual Lifshitz-Kosevich formula to determine the effective carrier mass from the temperature dependence of the amplitude of the oscillations will *overestimate the effective mass by the factor of three*. In fact, there have been conflicting experimental reports about the value of the effective mass for carriers in the electron pocket and the above circumstance may be relevant to this discrepancy. We expect that the temperature dependence of the oscillation amplitude may exhibit a crossover from $3X(T)e^{-3\pi/(\omega_c\tau)}/\sinh[3X(T)]$ at relatively low fields (when most electrons are paired, $H \lesssim H_{p2}$) to $X(T)e^{-\pi/(\omega_c\tau)}/\sinh[X(T)]$ at high fields (when most electrons are unpaired, $H \gg H_{p2}$).

IV. TWO-FLUID MODEL AND TRANSPORT PROPERTIES OF THE PSEUDO-GAP PHASE

Our main statement is that the pseudogap phase arises from the Fermi surface reconstruction induced by antiferromagnetic fluctuations into a holon Fermi surface in the nodal region and an electron pocket in the anti-nodal region. The latter electron pocket remains strongly paired (but uncondensed) up to very large energy scales, which may explain why the underlying single-electron excitations had escaped discovery until recently. The facts that the small electronic Fermi surface has been “visualized” in the quantum oscillation experiments only in a very narrow doping range and in just one class of materials are most likely related to the purity of the samples. In addition, the oscillations are observed in the vicinity of the “magic” doping fraction, $p = 1/8$, where it is known that stripe and other competing orders are enhanced, which therefore (according to the arguments of Sec. II) should suppress the energy scales for electron pairing and hence reduce the upper critical

field at which the oscillations are detectable. The latter argument is consistent with the observation of a dip in the superconducting dome in this doping region (we reiterate that the actual superconducting transition temperature, T_c , corresponds to Cooper pair condensation, which is different from the electron pairing temperature, T_p . However, the values of two temperature scales are expected to correlate strongly). It is therefore likely that even though the electron pocket has not so far been directly observed in quantum oscillation experiments and photoemission measurements in other doping regimes and other materials, it does exist throughout the phase diagram of the underdoped cuprates. Its elusive nature can be explained by the exponential suppression of the oscillations by the Dingle factor or/and much larger pairing energy scales away from the magic doping fraction.

Because the paired electron pocket is argued to be central to the phase diagram of the underdoped cuprates, it is important to discuss whether other unusual properties of the pseudogap phase (most importantly, its highly unusual transport properties) are consistent with the proposed mean-field state. In this section we argue that indeed many such anomalous thermal and electric transport experiments of the pseudogap phase can be qualitatively understood within our picture. In particular, as proposed in the early work of Geshkenbein *et al.*,¹⁷ a change of sign in transverse thermoelectric response can appear naturally within the corresponding two-fluid model of a $-2e$ Cooper pair Bose-liquid and the $+e$ hole Fermi liquid. Here, we discuss a complementary formulation of this model by ‘dualizing’ the bosons into vortices, while retaining the gapless fermionic excitations of the hole Fermi surface. Note that monopole Berry phases in \mathcal{L}_A (see Appendix A 4) are likely to play an important role in the vortex action,^{73,83} particularly in the structure of any charge order instabilities, but we will neglect this complication here.

Among the most unusual experiments in the pseudogap phase are the Hall and Nernst measurements. Here we qualitatively discuss these two effects within our two-fluid model of paired electrons and unpaired holon excitations. For completeness, we discuss in Appendix B the Hall conductivity of a generic anisotropic Fermi liquid. There are also corresponding expressions for the Nernst coefficient, as reviewed in Ref. 95. In Appendices C and D, we review the dual mapping procedure and formally derive the conductivity composition rule of a vortex-holon two-fluid model:

$$\hat{\sigma} = \frac{(2e)^2}{h} \hat{\sigma}_V^{-1} + \hat{\sigma}_f, \quad (4.1)$$

where $\hat{\sigma}_V$ is the dimensionless vortex conductivity matrix and $\hat{\sigma}_f$ is the electrical conductivity matrix of negatively charged holons. Eqs. (4.1) has the simple physical interpretation: In the pseudogap phase, the electrons are paired but uncondensed, which means that Cooper-pair conductivity, $\hat{\sigma}_{CP}$, is finite and is given by the vortex resistivity in the dual language.⁹⁶ The total conductivity is obtained simply by adding up the Cooper pair (or vortex) and the holon Fermi-liquid contribution, which leads to Eq. (4.1). Using this equation, we get the following expression for the Hall angle (see also, Ref. [97], where this equation was first

derived in a different context):

$$\tan \theta_H = \frac{\sigma_V^\perp + \sigma_f^\perp \text{Tr} \hat{\sigma}_V}{\sigma_V^\parallel + \sigma_f^\parallel \text{Tr} \hat{\sigma}_V}, \quad (4.2)$$

where $\text{Tr} \hat{\sigma}_V = (\sigma_V^\perp)^2 + (\sigma_V^\parallel)^2$. We see that both the magnitude and the sign of the Hall response are determined by the numerator of Eq. (4.2), which involves several physically distinct contributions that may and most likely do have opposite signs. While the sign of holon Hall conductivity is determined by that of the positive hole electric charge, the sign of the vortex contribution is expected to be opposite at least in the strong coupling regime. Indeed, assuming a dilute density of electronic tightly bound pairs, we expect them to behave like canonical bosons with charge $(-2e)$, and so contribute a negative Hall conductivity — this is the basic picture of Geshkenbein *et al.*¹⁷

The issue of the vortex Hall angle becomes more settled in the regime away from strong coupling. We emphasize here that by the “vortex” transport, here we are referring to the contribution of the electron pockets, whose normal state transport is described in a dual model of vortices. Within the framework of BCS theory, vortex conductivity has been considered previously by Dorsey⁹⁸ on the basis of the time-dependent Ginzburg-Landau equation, which for the case of our electronic pocket reads

$$\gamma (\partial_t - 2iea_\tau) \Delta_g = \frac{\hbar^2}{4m^*} (\nabla + 2ie\mathbf{a})^2 \Delta_g + \alpha \Delta_g - \beta |\Delta_g|^2 \Delta_g, \quad (4.3)$$

where $\Delta_g(t, \mathbf{r}) = \lambda_{\text{eff}} \langle g_+ g_- \rangle$ is the electronic Cooper-pair wave-function, α and β are the Landau parameters, and $\gamma = \gamma_1 + i\gamma_2$ is the order-parameter relaxation time. We note here that the time-dependent Ginzburg-Landau theory formally has a very narrow regime of applicability and is expected to be quantitatively valid only in the gapless superconductivity region. However, it should provide a useful insight about the vortex Hall contribution in the crossover from strong to weak coupling. According to Dorsey,⁹⁸ the vortex Hall angle is related in a complicated way to the relaxation parameter, γ , and the structure of the vortex core. But generally the sign of the Hall angle (relative to that in the normal phase) is determined by the sign of the following parameter, $(-\gamma_2/\gamma_1)$. In the clean limit of unscreened intervortex interactions (neutral superfluid) the situation simplifies leading to $\gamma = -i$ (which basically “restores” the Gross-Pitaevskii-like equation for the Cooper pair fluctuations) and giving the sign of the Hall angle identical to that in the normal phase, which is consistent with the discussion above in terms of the canonical bosons; the importance of this canonical boson contribution to the Hall transport was pointed out by Geshkenbein *et al.*¹⁷. In the weak-coupling and dirty limit, the situation is different and the sign of the Hall angle is determined by the Ginzburg-Landau time relaxation parameter given by (here we present

the result of the BCS model; see, *e.g.*, Aronov *et al.*:⁹⁹)

$$\gamma = \frac{\pi}{8} - \frac{iT_p}{2} \frac{\partial \ln T_p}{\partial \mu}. \quad (4.4)$$

Note that the BCS weak-coupling limit is not directly applicable to the strongly-paired electron pocket. However, Eq. (4.4) above provides a tentative indication that upon approaching the regime of weak Cooper pairing (*e.g.*, in the phase with enhanced antiferromagnetism correlations), the sign of the vortex Hall response may change. According to Eq. (4.4), it is determined by the value of logarithmic derivative of the BCS pairing temperature with respect to the chemical potential, which is proportional to the derivative of the density of states at the underlying Fermi surface (in our case, the Fermi surface of the electron pocket); depending upon the shape of the Fermi surface, this could have a negative sign. Therefore, in the weak coupling limit, the signs of the Hall contributions for the $h/(-2e)$ -vortices and $(+e)$ -holons may become the same (which could, in principle, be relevant in the vicinity of the “magic doping level,” where competing magnetic orders are enhanced leading presumably to a suppression of electron pairing, and where the change of sign in the Hall response has been observed). We reiterate however that the electron pocket is expected to remain strongly paired in the most, possibly all, of the pseudogap phase and therefore generally the vortex contribution is expected to retain the electron-like sign and to compete with the holon contribution.

The overall sign in the experimentally observed Hall effect will therefore be determined by the interplay of two physically different terms, σ_V^\perp and σ_f^\perp , and can show reversals depending on the system parameters. Again, in the proximity to the “magic” doping level, one expects decreased disorder (*i.e.*, decreased pinning strength) and suppression of the electron pairing as well, which should significantly alter the vortex contribution. We note that Taillefer *et al.*³² have reported a strong correlation between the sign-reversal in the Hall effect and the presence of quantum oscillations, which is qualitatively consistent with the afore-mentioned scenario.

In the simplest application of the two-fluid model, the Nernst effect will be determined by the contribution of the $h/(-2e)$ -vortices and the holons. However, in reality the situation may be more complicated due to a strong (possibly competing) effect of the superconducting fluctuations¹⁰³ (here we imply Aslamazov-Larkin amplitude fluctuations), which are known to be large compared to the Fermi-liquid terms even far above the pairing transition. Furthermore, possible charge-ordering instabilities of the vortex liquid,⁴³ and the associated proximity to the insulating state at $p = 1/8$ likely also play a role.⁴⁴

V. CONCLUSIONS

This paper has combined insights from recent experiments^{1,2,3,4,5,6,7,8,9,27,28,29,30,31,32} and earlier theoretical developments^{17,24,25,26} to present a fairly simple model for the underdoped cuprates with a firm microscopic and theoretical foundation. We start with a Fermi liquid state with long-range SDW order, containing electron pockets near the \mathbf{G}_a wavevectors, and hole pockets near the \mathbf{K}_v wavevectors (see Fig. 1). Then we express the spin polarization of the electronic excitations near these pockets in terms of the *local* polarization of the SDW order; this is the content of Eqs. (2.2) and (2.4). The advantage of this procedure is that it allows to easily extend key aspects of the physics of the small pockets into the phase without long-range SDW order. In particular, it shows that the electronic excitations experience a long-range gauge force associated with an emergent U(1) gauge field \mathbf{A} .

A key feature of our theory is that the primary pairing instability is associated with electron-like pockets near the \mathbf{G}_a wavevectors. We showed that these pockets experience a strong attractive pairing force from the transverse gauge fluctuations, and this leads naturally to an *s*-wave pairing instability. However, after rotating back to the physical spin polarization direction via Eq. (2.4), the resulting paired state was found to have a *d*-wave pairing signature for the physical electrons. Next we focused attention on the Josephson couplings in Eq. (2.11) between the electron and hole pockets: we found that it induced a *p*-wave pairing of the holons, which was strongly frustrated by the gauge forces on the holons. Again, after rotating back to the physical electrons using Eq. (2.2), this very weakly paired holon state was found to have a *d*-wave pairing signature with nodal fermionic excitations. The “nodal-anti-nodal dichotomy” is a natural consequence of this theory, with very different pairing physics near the \mathbf{G}_a and \mathbf{K}_v .

Section III explored the nature of the SdH oscillations in the normal state induced by a strong magnetic field at low temperatures. We computed the nature of the suppression of these oscillations by gauge field and pairing fluctuations.

Section IV explored aspects of transverse transport in the finite temperature pseudogap phase. Here, we also discussed connections to the boson-fermion model of Geshkenbein *et al.*¹⁷.

We conclude by mentioning that to determine the correctness of our proposed theory for the underdoped cuprates, it would be essential to visualize the single-particle excitations in the electron pocket in other experiments, apart from the existing quantum oscillation measurements. Such new experiments should involve external perturbations, which *destroy superconducting pairing* in the electron pocket, without smearing out its small Fermi surface or altering the underlying magnetic or topological order that yields Fermi surface reconstruction. Due to the former limitation, high temperature and/or strong disorder are not appropriate for this purpose. Possible other means could be, *e.g.*, to study AC transport in a magnetic field, looking, in particular, for cyclotron resonance effects coming from the single-electron excitations. Since the quantum oscillations have been observed, the mate-

rials are sufficiently clean to exhibit the cyclotron resonance phenomena as well. Another promising avenue could be to experimentally investigate *non-linear* transport, *e.g.*, non-linear IV -curves in a magnetic field. In the vicinity of the upper critical field $H_{p2}(T)$, the critical (depairing) current is expected to be relatively small and some manifestations of single-electron physics would appear at *lower fields* as compared to linear transport. Of particular interest would be also to compare the behavior of non-linear IV -curves in the regions with the opposite signs of the Hall conductivity. In our theory, the sign reversal in Hall response occurs naturally due to the competing contributions from the uncondensed electronic Cooper pairs and holons. This competition combined with the effects of depairing may lead a non-monotonic behavior and, possibly, sign reversals in non-linear transport data.

Acknowledgments

We are very grateful to Ady Stern for a discussion in which he pointed out the connection to the pairing problem in double layers of $\nu = 1/2$ quantum Hall systems.^{67,68} We thank Seamus Davis, Dennis Drew, Antoine Georges, Rick Greene, Andreas Hackl, Lev Ioffe, Yong-Baek Kim, Markus Müller, John-Pierre Paglione, Suchitra Sebastian, Z.-X. Shen, Tudor Stanescu, and Louis Taillefer for useful discussions. VG acknowledges the NSF Physics Frontier Center at JQI. The research of SS was supported by the NSF under grant DMR-0757145 and by the FQXi foundation.

APPENDIX A: COMPLETE LAGRANGIAN

Only two of the terms in the Lagrangian in Eq. (2.5), \mathcal{L}_g and \mathcal{L}_{fg} , were displayed in the body of the paper. This appendix will display the remaining terms, along with a brief discussion of their physical consequences.

1. Spinons

The Lagrangian for the z_α is²⁴

$$\mathcal{L}_z = |(\partial_\mu - iA_\mu)z_\alpha|^2 + s|z_\alpha|^2 + \frac{u}{2}(|z_\alpha|^2)^2, \quad (\text{A1})$$

and the spinon “mass” term s tunes a transition from the SDW ordered state ($\langle z_\alpha \rangle \neq 0$) to a state with spin rotation invariance preserved ($\langle z_\alpha \rangle = 0$). Note that in the SDW ordered state, the spinon condensate induces a Higgs “mass” term, $|\langle z_\alpha \rangle|^2 A_\mu^2$, for the A_μ .

2. Holons

These are associated with the $F_{v\alpha}$ fermionic excitations near the \mathbf{K}_v wave-vectors²⁵

$$\mathcal{L}_f = \sum_{q=\pm} \sum_{p=1,2} f_{qp}^\dagger \left[\partial_\tau - iqA_\tau - iea_\tau + \mu - E_{fg} - \frac{(\partial_{\bar{j}} - iqA_{\bar{j}} - iea_{\bar{j}})^2}{2m_{p\bar{j}}} \right] f_{qp}, \quad (\text{A2})$$

where \bar{j} extends over \bar{x}, \bar{y} , $m_{1\bar{x}} = m_{2\bar{y}}$ and $m_{2\bar{x}} = m_{1\bar{y}}$ are the masses of the elliptical holon pockets, and the \bar{x} and \bar{y} directions are rotated by 45° from the principle square axes. Eq. (A2) also contains the energy E_{fg} , which is the analog of the ‘‘semiconductor’’ band gap, between the top of the hole (valence) band and the bottom of the electron (conduction) band. We expect that the value of E_{fg} is sensitive to the strength of the SDW order, decreasing as the SDW order becomes larger.

3. Spin-charge couplings

These couple the spinons z_α to the holons $f_{\pm p}$ and the doublons g_\pm . The simplest allowed terms are couplings between the scalar densities, $|z_\alpha|^2$ and $f_{qp}^\dagger f_{\pm p}$, $g_\pm^\dagger g_\pm$. However, there are also ‘‘Shraiman-Siggia’’ terms⁵⁶ which couple operators carrying charges ± 2 under A_μ . Again, the most general form of all these terms can be deduced from the PSG, as has been described in previous works. For the holons, the spin-charge couplings take the form

$$\mathcal{L}_{zf} = \lambda_{zf} |z_\alpha|^2 \sum_{qp} f_{qp}^\dagger f_{qp} + i\tilde{\lambda}_{zf} \varepsilon^{\alpha\beta} \left\{ f_{+1}^\dagger f_{-1} z_\alpha \partial_{\bar{x}} z_\beta + f_{+2}^\dagger f_{-2} z_\alpha \partial_{\bar{y}} z_\beta \right\} + \text{H.c.} \quad (\text{A3})$$

The second term is the Shraiman-Siggia term; in the SDW state, this term favors incommensurate spiral spin correlations. In the non-magnetic state with $\langle z_\alpha \rangle = 0$, this term moves the electron spectral weight away from the commensurate \mathbf{K}_v points, to be centered on a ‘‘Fermi arc’’, as has been described in previous work.²⁴ Finally, integrating out the z_α also leads to an attractive pairing term¹⁰⁰ for the $f_{\pm p}$. For the g_\pm , the spin-charge couplings are

$$\begin{aligned} \mathcal{L}_{zg} = & \lambda_{zg} |z_\alpha|^2 \sum_q g_q^\dagger g_q \\ & + \tilde{\lambda}_{zg} \left\{ \varepsilon^{\alpha\beta} \left[g_+^\dagger (D_x g_-) z_\alpha (D_x^- z_\beta) - g_+^\dagger (D_y g_-) z_\alpha (D_y z_\beta) \right] \right. \\ & \left. + \varepsilon_{\alpha\beta} \left[g_-^\dagger (D_y g_+) z^{\alpha*} (D_y z^{\beta*}) - g_-^\dagger (D_x g_+) z^{\alpha*} (D_x z^{\beta*}) \right] \right\} + \text{H.c.} \end{aligned} \quad (\text{A4})$$

Now the Shraiman-Siggia term has 2 spatial gradients and does not induce spiral correlations.

4. Gauge field

These are induced by integrating out the matter fields, and can take a different form depending upon the nature of the matter excitations. When Fermi surfaces for g_{\pm} are present, the gauge field dynamics is overdamped, as discussed in the body of the paper. However, in all phases, terms of the form $\mathcal{L}_A \sim (\partial_{\mu}A_{\nu} - \partial_{\nu}A_{\mu})^2$ are always allowed, obtained by integrating high energy degrees of the freedom. For the crossover to the confining state, we also need to consider topologically non-trivial configurations of the A_{μ} corresponding to monopole tunnelling events. These have been ignored in the present paper because the monopoles are suppressed by the holon Fermi surfaces, but their effects have been discussed earlier^{24,25,26} in some detail. The monopoles come with Berry phases, and these are crucial in determining the nature of translational symmetry breaking in the confining phases.

APPENDIX B: HALL EFFECT IN AN ANISOTROPIC FERMIL LIQUID

In this appendix, we summarize the properties of transverse thermoelectric linear response in a two-dimensional anisotropic Fermi liquid and present a general expression for the Hall coefficient. The results presented in this appendix are used in Sec. IV, where the transverse thermoelectric response in the pseudogap phase is discussed.

Consider a two-dimensional Fermi liquid with the anisotropic dispersion $E = E(\mathbf{p})$. We also introduce the following standard notation: $\xi(p, \phi_{\mathbf{p}}) = E(p, \phi_{\mathbf{p}}) - E_{\text{F}}$, where $\mathbf{p} = (p, \phi_{\mathbf{p}})$ is simply the momentum in polar coordinates and E_{F} is the Fermi energy. This indirectly determines the value of the particle momentum as the function of energy and angle: $p = p(\xi, \phi_{\mathbf{p}})$. One can also define the particle velocity as a function of the energy and the angle: $\partial E / \partial p_{\alpha} = v_{\alpha}(\xi, \phi_{\mathbf{p}})$. We now introduce the following identity to treat the integrals over momentum [below, $F(\mathbf{p})$ is arbitrary function]

$$I_{\text{F}} = g_{\text{s}} \int \frac{d^2p}{(2\pi)^2} F(\mathbf{p}) = \int d\xi \langle \nu(\xi, \phi_{\mathbf{p}}) F(\xi, \phi_{\mathbf{p}}) \rangle, \quad (\text{B1})$$

where g_{s} is a degeneracy due to an internal degree of freedom (*e.g.*, spin in a usual electron liquid or a sublattice index in our theory), $\langle \dots \rangle = \int_0^{2\pi} (d\phi/2\pi) \dots$ is the average over the directions in the Brillouin zone (which reduces to the average over the Fermi surface if $\xi = 0$), and we introduced the density of states:

$$\nu(\xi, \phi_{\mathbf{p}}) = \frac{g_{\text{s}}}{4\pi} \frac{\partial}{\partial \xi} p(\xi, \phi_{\mathbf{p}}). \quad (\text{B2})$$

Let us also introduce the following notation for the integral that often appears in deriving

the finite temperature transport properties of a Fermi liquid:

$$[f(\varepsilon)]_T = \int_{-\infty}^{\infty} \frac{d\varepsilon}{4T} \frac{f(\varepsilon)}{\cosh^2\{\varepsilon/(2T)\}}. \quad (\text{B3})$$

At zero temperature, it simply gives $[f(\varepsilon)]_{T \rightarrow 0} = f(0)$. The notations defined by Eqs. (B1), (B2), and (B3) will be used below to express the general thermoelectric response coefficients in a compact and intuitive form, which would allow a simple physical interpretation.

The general theory of the Hall coefficient within the Green's function formalism has been considered by many authors and we refer the reader to the corresponding literature (see, *e.g.*, Altshuler and Aronov [101] and Livanov [102]). In the general case of an anisotropic Fermi liquid with an angle-dependent scattering time, $\tau_{\phi_{\mathbf{p}}}(\varepsilon)$, one can obtain the following expression for the Hall conductivity in the limit of a weak magnetic field (*i.e.*, if $\langle \omega_c \tau \rangle \ll 1$):

$$\sigma_{\alpha\beta}^{\perp} = e^3 H \left[\left\langle \tau_{\phi_{\mathbf{p}}}^2(\varepsilon) \frac{\partial}{\partial \varepsilon} \{v_{\alpha}^2(\varepsilon, \phi_{\mathbf{p}}) v_{\beta}^2(\varepsilon, \phi_{\mathbf{p}}) \nu(\varepsilon, \phi_{\mathbf{p}})\} \right\rangle \right]_T. \quad (\text{B4})$$

In the zero temperature limit, $T/E_F \rightarrow 0$, and assuming an angle-independent scattering time, τ , we get the simplified equation for the Hall response ($\alpha \neq \beta$):

$$\sigma_{\alpha\beta}^{\perp} = e^3 \tau^2 H \left\langle \frac{\partial}{\partial \varepsilon} \{v_{\alpha}^2 v_{\beta}^2 \nu\} \right\rangle_{\text{FS}}. \quad (\text{B5})$$

The corresponding expression for the longitudinal Drude conductivity is

$$\sigma_{\alpha\alpha}^{\parallel} = e^2 \tau \langle v_{\alpha}^2 \nu \rangle_{\text{FS}}. \quad (\text{B6})$$

In the isotropic limit of a circular Fermi surface, $v^2 = 2E/m$, and Eq. (B5) reproduces the familiar expression for the Hall conductivity $\sigma^{\perp} = (\omega_c \tau) \sigma^{\parallel}$, with $\sigma^{\parallel} = (v_F^2/2) \nu e^2 \tau$ being the longitudinal Drude conductivity of Eq. (B6). We emphasize here that according to Eq. (B5), the Hall coefficient does depend on the derivative of the density of states, but the latter effects are not necessarily dominant. *E.g.*, the Hall conductivity is finite even if the density-of-states is a constant. The sign of the Hall effect can change within a single-band Fermi liquid picture only if the density-of-states depends on the energy stronger than $v_x^2 v_y^2$ in the corresponding directions, which requires a very anisotropic Fermi surface.

APPENDIX C: DUALITY TRANSFORMATION

The mean-field Lagrangian of this two-fluid model can be written as follows:

$$\mathcal{L}[\Delta_g, f] = \mathcal{L}_{\text{GL}}[\Delta_g] + \mathcal{L}_{\text{h}}[f] + \mathcal{L}_{\text{J}}[\Delta_g, f], \quad (\text{C1})$$

where $\Delta_g = \lambda_{\text{eff}} \langle g_+ g_- \rangle$ is the pairing order parameter describing electron Cooper pairs and \mathcal{L}_{GL} is the corresponding Ginzburg-Landau Lagrangian

$$\mathcal{L}_{\text{GL}}[\Delta_g] = \Delta_g^* \left[\frac{(-i\nabla - 2e\mathbf{a})^2}{4m} + (\partial_\tau - 2iea_\tau) \right] \Delta_g + \alpha(T) |\Delta_g|^2 - \beta |\Delta_g|^4, \quad (\text{C2})$$

where $a = (a_\tau, \mathbf{a})$ is the physical electromagnetic field (we assumed that all effects of the gauge field, A , have already been incorporated into the effective parameters) and α and β are Ginzburg-Landau parameters, which determine the modulus of the order parameter, $|\Delta_g| \equiv \Delta_0 = \sqrt{\alpha/(2\beta)}$, which we assume fixed. However, the phase, ϕ , of the order parameter, $\Delta_g = \Delta_0 \exp(i\phi)$, is allowed to fluctuate. This leads to the XY-model for the electronic Cooper pairs and a Kosterlitz-Thouless transition below the BCS pairing temperature, T_{p0} . The second term in Eq. (C1) is the free fermion Lagrangian describing the motion of holes

$$\mathcal{L}_{\text{h}}[f] = f^* \left[\frac{(-i\nabla + e\mathbf{a})^2}{2m_h} + (\partial_\tau + iea_\tau) \right] f, \quad (\text{C3})$$

where the term $(+e\mathbf{a})$ describes coupling of the holes to the electromagnetic field. Finally, the last term in Eq. (C1), $\mathcal{L}_{\text{J}}[\Delta_g, f]$, is given by Eq. (2.11) and describes internal tunnelling between the electrons and the holes.

The structure of the tunnelling term is given by $e^{i\phi} f f$, and it is very similar to that in the usual BCS mean-field model of a gapless superconductor (see, *e.g.*, Ref. [97]). One can therefore just follow the steps used in Refs. [97,105] to derive the so-called $U(1)$ formulation¹⁰⁵ of the vortex-fermion mixture in this model, which describes the motion of vortices statistically coupled to gapless fermions: The statistical interaction is that they “see each other” as sources of a $(-\pi)$ -flux and therefore induce electromotive force on each other when moving. The first purely technical step is to introduce a new operator, $h_{\mathbf{r}} = e^{i\phi_{\mathbf{r}}/2} f_{\mathbf{r}}$, which simplifies the Josephson term. The next step is to perform a duality transformation with respect to the bosonic Cooper-pair field, $e^{i\phi_{\mathbf{r}}}$. The resulting action describing a two-fluid vortex-holon liquid is

$$\mathcal{L}[\Psi_V, h] = \Psi_V^* \left[\frac{(-i\nabla - \mathbf{a}^{\text{dual}} + \boldsymbol{\alpha})^2}{2M_V} + (\partial_\tau + ia_\tau^{\text{dual}} + i\alpha_\tau) \right] \Psi_V \quad (\text{C4})$$

$$+ h^* \left[\frac{(-i\nabla - \boldsymbol{\beta})^2}{2m_h} + (\partial_\tau - i\beta_\tau) \right] h + \mathcal{L}_{\text{gauge}}, \quad (\text{C5})$$

where M_V is a vortex mass, a^{dual} is the gauge field, which describes the Cooper pair density fluctuations [$\nabla \times \mathbf{a}^{\text{dual}} = n_{\text{CP}}(\mathbf{r})$], and the only purpose of the fields α and β is to mediate the long-range statistical interaction between the vortices and the fermions. These fields are “attached” to the vortices via $\nabla \times \boldsymbol{\beta} = i\pi\Psi_V^\dagger\Psi_V$ and to the fermions via $\nabla \times \boldsymbol{\alpha} = i\pi h^\dagger h$

This statistical interaction is described by the mutual Chern-Simons term, which is the first term in the following gauge part of the action

$$\mathcal{L}_{\text{gauge}} = -\frac{i}{\pi} (\epsilon_{\mu\nu\lambda} \alpha_\mu \partial_\nu \beta_\lambda) + \frac{1}{2C} (\epsilon_{\mu\nu\lambda} \partial_\nu a_\lambda^{\text{dual}} - \delta_{\mu 0} 2\pi n_0)^2 + \frac{i}{2\pi} J_\mu^{\text{cp}} \epsilon_{\mu\nu\lambda} \partial_\nu a_\lambda^{\text{dual}}. \quad (\text{C6})$$

The second term in Eq. (C6) describes dual gauge-field fluctuations, which physically correspond to plasmons. In a charged system, the plasmons have a gap due to the long-range Coulomb forces and as such the fluctuations of this gauge field are expected to be less pronounced than in a neutral Bose-system. Finally, the last term describes coupling to a physical electric Cooper pair current.

The theory of Eqs. (C4) and (C6) summarizes the following essential features of the two-fluid vortex-holon mixture: The vortices and the Cooper pairs “see each other” as $(+2\pi)$ -fluxes and induce EMFs (transverse Magnus forces) on each other when moving. Likewise, the vortices and the gapless fermions (holons) “see each other” as $(-\pi)$ -fluxes and induce EMFs as well. We will be using this picture in derivation of the semiclassical transport equations below.

A more settled issue is the question of the total effective magnetic field (“dual field”) seen by a vortex. According, to Eqs. (C4) and (C6), it is $B^{(\text{dual})} = \nabla \times [\mathbf{a}^{(\text{dual})} - \boldsymbol{\alpha}] = 2\pi (n_0 - \frac{1}{2}n_h)$. We reiterate that the Josephson term (2.11) in the action violates the individual conservation laws for the g - and f -particles. This means in particular that the density of the latter, n_h , may vary depending on the phase. Another related non-trivial question is about the vortex statistics (with respect to each other). The direct duality transformation gives bosonic vortices, however other statistics are in principle possible. These are very interesting questions, which however are beyond the scope of the present study. Below, we treat the vortices semiclassically to develop a phenomenological theory of transport and derive the corresponding transport coefficients.

APPENDIX D: CONDUCTIVITY COMPOSITION RULE IN THE TWO-FLUID VORTEX-HOLON MODEL

The derivation of the semiclassical theory of transport in the two-fluid model is essentially identical to that of Ref. [97] and is based on the following equations, which describe the electromotive forces between the vortices, fermions, and Cooper pairs in the presence of currents and thermal gradients:

$$\begin{aligned} \mathbf{j}_v &= -\hat{\sigma}_v \hat{\epsilon} (\mathbf{j}_h + \mathbf{j}_{\text{CP}}) - \hat{\lambda}_v \nabla T; \\ \mathbf{j}_h &= -\hat{\sigma}_h \hat{\epsilon} \mathbf{j}_v - \hat{\lambda}_h \nabla T, \end{aligned} \quad (\text{D1})$$

where $\hat{\epsilon}$ is the antisymmetric tensor in two dimensions, \mathbf{j}_v , \mathbf{j}_h , and \mathbf{j}_{cp} are the vortex, holon, and Cooper pair density currents respectively and $\hat{\sigma}_{v/h}$ and $\hat{\lambda}_v$ are the vortex/holon di-

mensionless conductance and thermal conductivity matrices respectively. The latter two matrices generally have the form

$$\sigma = \begin{pmatrix} \sigma_{\parallel} & \sigma_{\perp} \\ -\sigma_{\perp} & \sigma_{\parallel} \end{pmatrix} \quad \text{and} \quad \lambda = \begin{pmatrix} \lambda_{\parallel} & \lambda_{\perp} \\ -\lambda_{\perp} & \lambda_{\parallel} \end{pmatrix}. \quad (\text{D2})$$

The quantities of interest are the total electrical and thermal conductivity matrices for the system. *E.g.*, in the absence of thermal gradients, the conductivity tensor is defined by $\mathbf{j}_{\text{CP}} = \hat{\epsilon}\mathbf{E}$, while the actual electric field is determined by $\mathbf{E} = \frac{1}{2e}\hat{\epsilon}\mathbf{j}_v$. Then, Eqs. (D1) can be easily resolved and give the following expression for the total electrical conductivity matrix:

$$\hat{\sigma} = (2e)^2 \left[\hat{\sigma}_v^{-1} + \frac{1}{4}\hat{\sigma}_h \right]. \quad (\text{D3})$$

Despite the rather complicated set of arguments and transformation that have led to this result, the physics of Eq. (D3) is very simple: The total electrical conductivity in the uncondensed liquid phase is given by the sum of Cooper pair and hole conductivities. The former can be related to the vortex transport properties and due to duality is simply given by the vortex resistivity. One can also derive a complete phenomenological expression for the Peltier tensor in the two-fluid model defined via $\mathbf{E} = \hat{\lambda}\nabla T$. The exact expression for the Peltier tensor is rather involved, but assuming that the hole contribution to the Nernst effect is negligible, one can use the results of Ref. [97].

-
- ¹ K. M. Shen, F. Ronning, D. H. Lu, F. Baumberger, N. J. C. Ingle, W. S. Lee, W. Meevasana, Y. Kohsaka, M. Azuma, M. Takano, H. Takagi, and Z.-X. Shen, *Science* **307**, 901 (2005).
 - ² A. Kanigel, M. R. Norman, M. Randeria, U. Chatterjee, S. Souma, A. Kaminski, H. M. Fretwell, S. Rosenkranz, M. Shi, T. Sato, T. Takahashi, Z. Z. Li, H. Raffy, K. Kadowaki, D. Hinks, L. Ozyuzer, J. C. Campuzano, *Nature Physics* **2**, 447 (2006).
 - ³ M. Le Tacon, A. Sacuto, A. Georges, G. Kotliar, Y. Gallais, D. Colson, and A. Forget, *Nature Physics* **2**, 537-543 (2006).
 - ⁴ K. Tanaka, W. S. Lee, D. H. Lu, A. Fujimori, T. Fujii, Risdiana, I. Terasaki, D. J. Scalapino, T. P. Devereaux, Z. Hussain, and Z.-X. Shen, *Science* **314**, 1910 (2006).
 - ⁵ Y. Kohsaka, C. Taylor, K. Fujita, A. Schmidt, C. Lupien, T. Hanaguri, M. Azuma, M. Takano, H. Eisaki, H. Takagi, S. Uchida, and J. C. Davis, *Science* **315**, 1380 (2007).
 - ⁶ M. C. Boyer, W. D. Wise, Kamallesh Chatterjee, Ming Yi, Takeshi Kondo, T. Takeuchi, H. Ikuta, E. W. Hudson, *Nature Physics* **3**, 802 (2007)
 - ⁷ Y. Kohsaka, C. Taylor, P. Wahl, A. Schmidt, Jinhwan Lee, K. Fujita, J. W. Alldredge, K. McElroy, Jinho Lee, H. Eisaki, S. Uchida, D.-H. Lee, and J. C. Davis, *Nature* **454**, 1072

- (2008).
- ⁸ J.-H. Ma, Z.-H. Pan, F. C. Niestemski, M. Neupane, Y.-M. Xu, P. Richard, K. Nakayama, T. Sato, T. Takahashi, H.-Q. Luo, L. Fang, H.-H. Wen, Ziqiang Wang, H. Ding, and V. Madhavan, *Phys. Rev. Lett.* **101**, 207002 (2008).
 - ⁹ S. Huefner, M. A. Hossain, A. Damascelli and G. A. Sawatzky, *Rep. Prog. Phys.* **71**, 062501 (2008).
 - ¹⁰ S. Sachdev, A. V. Chubukov, and A. Sokol, *Phys. Rev. B* **51**, 14874 (1995).
 - ¹¹ A. V. Chubukov and D. K. Morr, *Physics Reports* **288**, 355 (1997).
 - ¹² A. J. Millis and M. R. Norman, *Phys. Rev. B* **76**, 220503 (2007).
 - ¹³ N. Harrison, arXiv:0902.2741.
 - ¹⁴ C. Honerkamp, M. Salmhofer, N. Furukawa, and T. M Rice, *Phys. Rev. B* **63**, 035109 (2001).
 - ¹⁵ D. Senechal and A.-M. S. Tremblay, *Phys. Rev. Lett.* **92**, 126401, (2004).
 - ¹⁶ M. Civelli, M. Capone, S. S. Kancharla, O. Parcollet, and G. Kotliar, *Phys. Rev. Lett.* **95**, 106402 (2005).
 - ¹⁷ V. B. Geshkenbein, L. B. Ioffe, and A. I. Larkin, *Phys. Rev. B* **55**, 3173 (1997).
 - ¹⁸ R. M. Konik, T. M. Rice, and A. M. Tsvelik, *Phys. Rev. Lett.* **96**, 086407 (2006).
 - ¹⁹ Kai-Yu Yang, T. M. Rice, and Fu-Chun Zhang, *Phys. Rev. B* **73**, 174501 (2006).
 - ²⁰ A. M. Tsvelik and A. V. Chubukov, *Phys. Rev. Lett.* **98**, 237001 (2007).
 - ²¹ M. Oshikawa, *Phys. Rev. Lett.* **84**, 3370 (2000).
 - ²² T. Senthil, S. Sachdev, and M. Vojta, *Phys. Rev. Lett.* **90**, 216403 (2003).
 - ²³ T. Senthil, M. Vojta, and S. Sachdev, *Phys. Rev. B* **69**, 035111 (2004).
 - ²⁴ R. K. Kaul, A. Kolezhuk, M. Levin, S. Sachdev, and T. Senthil, *Phys. Rev. B* **75** , 235122 (2007).
 - ²⁵ R. K. Kaul, Y. B. Kim, S. Sachdev, and T. Senthil, *Nature Physics* **4**, 28 (2008).
 - ²⁶ R. K. Kaul, M. A. Metlitski, S. Sachdev and C. Xu, *Phys. Rev. B* **78**, 045110 (2008).
 - ²⁷ N. Doiron-Leyraud, C. Proust, D. LeBoeuf, J. Levallois, J.-B. Bonnemaïson, R. Liang, D. A. Bonn, W. N. Hardy, and L. Taillefer, *Nature* **447**, 565 (2007).
 - ²⁸ E. A. Yelland, J. Singleton, C. H. Mielke, N. Harrison, F. F. Balakirev, B. Dabrowski, and J. R. Cooper, *Phys. Rev. Lett.* **100**, 047003 (2008).
 - ²⁹ A. F. Bangura, J. D. Fletcher, A. Carrington, J. Levallois, M. Nardone, B. Vignolle, P. J. Heard, N. Doiron-Leyraud, D. LeBoeuf, L. Taillefer, S. Adachi, C. Proust, and N. E. Hussey, *Phys. Rev. Lett.* **100**, 047004 (2008).
 - ³⁰ C. Jaudet, D. Vignolles, A. Audouard, J. Levallois, D. LeBoeuf, N. Doiron-Leyraud, B. Vignolle, M. Nardone, A. Zitouni, Ruixing Liang, D. A. Bonn, W. N. Hardy, L. Taillefer, and C. Proust, *Phys. Rev. Lett.* **100**, 187005 (2008).
 - ³¹ S. E. Sebastian, N. Harrison, E. Palm, T. P. Murphy, C. H. Mielke, Ruixing Liang, D. A. Bonn, W. N. Hardy, and G. G. Lonzarich, *Nature* **454**, 200 (2008).
 - ³² D. LeBoeuf, N. Doiron-Leyraud, J. Levallois, R. Daou, J.-B. Bonnemaïson, N. E. Hussey,

- L. Balicas, B. J. Ramshaw, R. Liang, D. A. Bonn, W. N. Hardy, S. Adachi, C. Proust, and L. Taillefer, *Nature* **450**, 533 (2007).
- ³³ We are grateful to S. Sebastian for discussions on this point.
- ³⁴ E. Demler, S. Sachdev and Y. Zhang, *Phys. Rev. Lett.* **87**, 067202 (2001); Y. Zhang, E. Demler and S. Sachdev, *Phys. Rev. B* **66**, 094501 (2002).
- ³⁵ S. Katano, M. Sato, K. Yamada, T. Suzuki, and T. Fukase, *Phys. Rev. B* **62**, R14677 (2000).
- ³⁶ B. Lake, H. M. Rønnow, N. B. Christensen, G. Aeppli, K. Lefmann, D. F. McMorrow, P. Vorderwisch, P. Smeibidl, N. Mangkorntong, T. Sasagawa, M. Nohara, H. Takagi, and T. E. Mason, *Nature* **415**, 299 (2002).
- ³⁷ J. M. Tranquada, C. H. Lee, K. Yamada, Y. S. Lee, L. P. Regnault, and H. M. Rønnow, *Phys. Rev. B* **69**, 174507 (2004).
- ³⁸ B. Khaykovich, S. Wakimoto, R. J. Birgeneau, M. A. Kastner, Y. S. Lee, P. Smeibidl, P. Vorderwisch, and K. Yamada, *Phys. Rev. B* **71**, 220508 (2005).
- ³⁹ J. Chang, Ch. Niedermayer, R. Gilardi, N. B. Christensen, H. M. Rønnow, D. F. McMorrow, M. Ay, J. Stahn, O. Sobolev, A. Hiess, S. Pailhes, C. Baines, N. Momono, M. Oda, M. Ido, and J. Mesot, *Phys. Rev. B* **78**, 104525 (2008).
- ⁴⁰ J. Chang, N. B. Christensen, Ch. Niedermayer, K. Lefmann, H. M. Rønnow, D. F. McMorrow, A. Schneidewind, P. Link, A. Hiess, M. Boehm, R. Mottl, S. Pailhes, N. Momono, M. Oda, M. Ido, and J. Mesot, arXiv:0902.1191.
- ⁴¹ D. Haug, V. Hinkov, A. Suchaneck, D. S. Inosov, N. B. Christensen, Ch. Niedermayer, P. Bourges, Y. Sidis, J. T. Park, A. Ivanov, C. T. Lin, J. Mesot, and B. Keimer, arXiv:0902.3335.
- ⁴² Wei-Qiang Chen, Kai-Yu Yang, T. M. Rice, and F. C. Zhang, *EuroPhys. Lett.* **82**, 17004 (2008).
- ⁴³ L. Balents, L. Bartosch, A. Burkov, S. Sachdev, and K. Sengupta, *Phys. Rev. B* **71**, 144508 (2005).
- ⁴⁴ S. A. Hartnoll, P. K. Kovtun, M. Müller, and S. Sachdev, *Phys. Rev. B* **76**, 144502 (2007).
- ⁴⁵ P. W. Anderson, P. A. Lee, M. Randeria, T. M. Rice, N. Trivedi, and F. C. Zhang, *J. Phys. Condens. Matter* **16**, R755-R769 (2004).
- ⁴⁶ N. P. Armitage, D. H. Lu, C. Kim, A. Damascelli, K. M. Shen, F. Ronning, D. L. Feng, P. Bogdanov, X. J. Zhou, W. L. Yang, Z. Hussain, P. K. Mang, N. Kaneko, M. Greven, Y. Onose, Y. Taguchi, Y. Tokura, and Z.-X. Shen, *Phys. Rev. B* **68**, 604517 (2003).
- ⁴⁷ T. Claesson, M. Månsson, C. Dallera, F. Venturini, C. De Nadaï, N. B. Brookes, and O. Tjernberg, *Phys. Rev. Lett.* **93**, 136402 (2004).
- ⁴⁸ H. Matsui, K. Terashima, T. Sato, T. Takahashi, S.-C. Wang, H.-B. Yang, H. Ding, T. Uefuji, and K. Yamada, *Phys. Rev. Lett.* **94**, 047005 (2005).
- ⁴⁹ S. R. Park, Y. S. Roh, Y. K. Yoon, C. S. Leem, J. H. Kim, B. J. Kim, H. Koh, H. Eisaki, N. P. Armitage, and C. Kim, *Phys. Rev. B* **75**, 060501(R) (2007).

- ⁵⁰ Y. Qi and S. Sachdev, Phys. Rev. B **77**, 165112 (2008), Section IV.
- ⁵¹ A. Comanac, L. de' Medici, M. Capone, and A. J. Millis, Nature Physics **4**, 287 (2008).
- ⁵² A. W. Sandvik, Phys. Rev. Lett. **98**, 227202 (2007).
- ⁵³ R. G. Melko and R. K. Kaul, Phys. Rev. Lett. **100**, 017203 (2008); Phys. Rev. B **78**, 014417 (2008).
- ⁵⁴ F.-J. Jiang, M. Nyfeler, S. Chandrasekharan, and U.-J. Wiese, arXiv:0710.3926.
- ⁵⁵ A. B. Kuklov, M. Matsumoto, N. V. Prokof'ev, B. V. Svistunov, and M. Troyer, Phys. Rev. Lett. **101**, 050405 (2008).
- ⁵⁶ B. I. Shraiman and E. D. Siggia, Phys. Rev. Lett. **61**, 467 (1988).
- ⁵⁷ E. Berg and E. Altman, Phys. Rev. Lett. **99**, 247001 (2007).
- ⁵⁸ X.-G. Wen, Phys. Rev. B **39**, 7223 (1989).
- ⁵⁹ P. A. Lee, Phys. Rev. Lett. **63**, 680 (1989).
- ⁶⁰ R. Shankar, Phys. Rev. Lett. **63**, 203 (1989).
- ⁶¹ L. B. Ioffe and P. B. Wiegmann, Phys. Rev. Lett. **65**, 653 (1990).
- ⁶² L. B. Ioffe and A. I. Larkin, Phys. Rev. B **39**, 8988 (1989).
- ⁶³ B. I. Halperin, P. A. Lee, and N. Read, Phys. Rev. B **47**, 7312 (1993).
- ⁶⁴ R. K. Kaul and S. Sachdev, Phys. Rev. B **77**, 155105 (2008).
- ⁶⁵ V. M. Galitski and Y.-B. Kim, Phys. Rev. Lett. **99**, 266403 (2007).
- ⁶⁶ S.-S. Lee, P. A. Lee, and T. Senthil, Phys. Rev. Lett. **98**, 067006 (2007).
- ⁶⁷ N. E. Bonesteel, I. A. McDonald, and C. Nayak, Phys. Rev. Lett. **77**, 3009 (1996).
- ⁶⁸ I. Ussishkin and A. Stern, Phys. Rev. Lett. **81**, 3932 (1998).
- ⁶⁹ D. J. Bergmann and D. Rainer, Z. Phys. **263**, 59 (1973).
- ⁷⁰ A. J. Millis, S. Sachdev, and C. M. Varma, Phys. Rev. B **37**, 4975 (1988).
- ⁷¹ R. Roussev and A. J. Millis, Phys. Rev. B **63**, 140504(R) (2001).
- ⁷² A. V. Chubukov, A. M. Finkel'stein, R. Haslinger, and D. K. Morr, Phys. Rev. Lett. **90**, 077002 (2003).
- ⁷³ L. Balents and S. Sachdev, Annals of Physics **322**, 2635 (2007).
- ⁷⁴ M. Yu. Kuchiev and O. P. Sushkov, Physica C **218**, 197 (1993).
- ⁷⁵ V. V. Flambaum, M. Yu. Kuchiev, and O. P. Sushkov, Physica C **227**, 267 (1994).
- ⁷⁶ V. I. Belinicher, A. L. Chernyshev, A. V. Dotsenko, and O. P. Sushkov Phys. Rev. B **51**, 6076 (1995).
- ⁷⁷ O. P. Sushkov and V. N. Kotov, Phys. Rev. B **70**, 024503 (2004).
- ⁷⁸ E. Helfand and N. R. Werthamer, Phys. Rev. Lett. **13**, 686 (1964); Phys. Rev. **147**, 288 (1966); E. Helfand, N. R. Werthamer, and P. C. Hohenberg, Phys. Rev. **147**, 295 (1966).
- ⁷⁹ V. M. Galitski and A. I. Larkin Phys. Rev. Lett. **87**, 087001 (2001)
- ⁸⁰ V. P. Mineev, Jour. Phys. Soc. Jpn. **69**, 3371 (2000).
- ⁸¹ V. M. Galitski and A. I. Larkin, Phys. Rev. B **63**, 174506 (2001); Phys. Rev. B **67**, 144501 (2003).

- ⁸² T. D. Stanescu, V. M. Galitski, and H. D. Drew, Phys. Rev. Lett. **101**, 066405 (2008).
- ⁸³ L. Balents, L. Bartosch, A. Burkov, S. Sachdev, and K. Sengupta, Phys. Rev. B **71**, 144509 (2005).
- ⁸⁴ L. B. Ioffe and G. Kotliar, Phys. Rev. B **42**, 10348 (1990).
- ⁸⁵ A. G. Aronov, E. Altshuler, A. D. Mirlin, and P. Wölfle, Phys. Rev. B **52**, 4708 (1995).
- ⁸⁶ A. D. Mirlin, E. Altshuler, and P. Wölfle, Annalen der Physik **5**, 281 (1996).
- ⁸⁷ L. W. Gruenberg and L. L. Günter, Phys. Rev. **176**, 606 (1968).
- ⁸⁸ V. P. Mineev, Physica B **1072**, 259 (1999).
- ⁸⁹ T. Champel and V. P. Mineev, Phil. Mag. B, **81**, 55 (2001).
- ⁹⁰ Note that our estimate of the Ginzburg parameter is for the small pockets of electrons, near the anti-nodal points. In contrast, Ref. 17 assumed these electrons had already paired into bosons. They estimated a very small Ginzburg parameter for the fermions near the Fermi arcs along the Brillouin zone diagonals; the pairing of these fermions is also relatively weak in our theory.
- ⁹¹ A. I. Larkin and A. A. Varlamov, *Theory of fluctuations in superconductors*, Oxford University Press (2005).
- ⁹² D. V. Livanov, G. Savona and A. A. Varlamov, Phys. Rev. **B**, 8675 (2000).
- ⁹³ L. G. Aslamazov and A. I. Larkin, Sov. Phys. Solid State, **10**, 875 (1968).
- ⁹⁴ S. Dukan and Z. Tešanović, Phys. Rev. Lett. **74**, 2311 (1995).
- ⁹⁵ A. Hackl and S. Sachdev, arXiv:0901.2348.
- ⁹⁶ M. P. A. Fisher Phys. Rev. Lett. **65**, 923 (1990).
- ⁹⁷ V. M. Galitski, G. Refael, M. P. A. Fisher, T. Senthil, Phys. Rev. Lett **95**, 077002 (2005).
- ⁹⁸ A. T. Dorsey, Phys. Rev. B **46**, 8376 (1992).
- ⁹⁹ A. G. Aronov, S. Hikami, and A. I. Larkin, Phys. Rev. B **51**, 3880 (1995)
- ¹⁰⁰ Ref. 50, Section V.
- ¹⁰¹ B. L. Altshuler and A. G. Aronov, “Electron-electron interactions in disordered systems,” ed. by M. Pollak and A. L. Efros, pp. 1-151, In: *Modern Problems in Condensed Matter Physics*, North Holland (1985).
- ¹⁰² D. V. Livanov, Phys. Rev. B **60**, 13439 (1999).
- ¹⁰³ M. N. Serbyn, M. A. Skvortsov, A. A. Varlamov, and V. M. Galitski, Phys. Rev. Lett. **102**, 067001 (2009).
- ¹⁰⁴ E. Sondheimer, Proc. Roy. Soc. (London) **A193**, 484 (1948).
- ¹⁰⁵ L. Balents and M. P. A. Fisher, Phys. Rev. B **71**, 085119 (2005).